



MYB sustains hypoxic survival of pancreatic cancer cells by facilitating metabolic reprogramming

Shashi Anand^{1,2}, Mohammad Aslam Khan^{1,2}, Haseeb Zubair^{1,2} , Sarabjeet Kour Sudan^{1,2}, Kunwar Somesh Vikramdeo^{1,2}, Sachin Kumar Deshmukh^{1,2}, Shafquat Azim^{1,2}, Sanjeev Kumar Srivastava^{1,2}, Seema Singh^{1,2,3} & Ajay Pratap Singh^{1,2,3,*} 

Abstract

Extensive desmoplasia and poor vasculature renders pancreatic tumors severely hypoxic, contributing to their aggressiveness and therapy resistance. Here, we identify the HuR/MYB/HIF1 α axis as a critical regulator of the metabolic plasticity and hypoxic survival of pancreatic cancer cells. HuR undergoes nuclear-to-cytoplasmic translocation under hypoxia and stabilizes MYB transcripts, while MYB transcriptionally upregulates HIF1 α . Upon MYB silencing, pancreatic cancer cells fail to survive and adapt metabolically under hypoxia, despite forced overexpression of HIF1 α . MYB induces the transcription of several HIF1 α -regulated glycolytic genes by directly binding to their promoters, thus enhancing the recruitment of HIF1 α to hypoxia-responsive elements through its interaction with p300-dependent histone acetylation. MYB-depleted pancreatic cancer cells exhibit a dramatic reduction in tumorigenic ability, glucose-uptake and metabolism in orthotopic mouse model, even after HIF1 α restoration. Together, our findings reveal an essential role of MYB in metabolic reprogramming that supports pancreatic cancer cell survival under hypoxia.

Keywords HIF1 α ; hypoxia; metabolic reprogramming; MYB; pancreatic cancer

Subject Categories Cancer; Metabolism; RNA Biology

DOI 10.15252/embr.202255643 | Received 23 June 2022 | Revised 13 December 2022 | Accepted 19 December 2022 | Published online 2 January 2023

EMBO Reports (2023) 24: e55643

Introduction

Pancreatic cancer (PC) is one of the most notorious malignancies, with a current five-year survival rate of about 10% (Siegel *et al*, 2022). It is characterized by poor vasculature and extensive desmoplasia that create highly hypoxic niches within the tumor microenvironment, enforcing the selection of adaptive tumor cell types (Hingorani *et al*, 2003; Feig *et al*, 2012; Dauer *et al*, 2017; Yamasaki *et al*, 2020). In response to hypoxia, cancer cells undergo a reprogramming of cellular and metabolic pathways to sustain their

survival and gain aggressive features (Eales *et al*, 2016; Hollinshead *et al*, 2020). Hypoxia-inducible factors (HIFs) act as the master regulators of hypoxia-activated gene expression and exhibit increased accumulation due to the inhibition of the proteasomal degradation (Semenza, 2013). HIF1 α is ubiquitously expressed, and several of its target genes encode for metabolic enzymes and membrane transporters that help tumor cells adapt metabolically under the hypoxic environment and promote its aggressive progression (Marin-Hernandez *et al*, 2009; Semenza, 2010, 2013). However, there is also evidence suggesting tumor suppressive functions of HIF1 α in some malignancies, including pancreatic cancer, suggesting a complex regulation of its activity by other tumor-associated proteins (Shen *et al*, 2011; Tiwari *et al*, 2020).

MYB is a proto-oncogene that encodes for a transcription factor protein involved in the gene regulation (Slamon *et al*, 1986). It is expressed in immature hematopoietic cells of all lineages and plays a role in maintaining their undifferentiated proliferative state (Greig *et al*, 2008). Previously, we demonstrated a significant role of MYB in pancreatic tumor growth and metastasis (Srivastava *et al*, 2015). We also showed that MYB promoted desmoplasia by potentiating the bi-directional crosstalk between pancreatic cancer and stellate cells (Singh *et al*, 2012). Further, the characterization of MYB-regulated gene networks and secretome in PC cells suggested its broader pathobiological implications (Azim *et al*, 2016; Zubair *et al*, 2020). An aberrant expression of MYB has been reported in several malignancies, including PC (Slamon *et al*, 1986; Wallrapp *et al*, 1997; Weston, 1999; Li *et al*, 2014, 2016; Srivastava *et al*, 2021). Various mechanisms have been implicated in MYB regulation in normal and malignant cells (Gudas *et al*, 1995; Dasse *et al*, 2012; George & Ness, 2014). Further, MYB is shown to act in concert with other proteins in a context-dependent manner to impact diverse biological functions (George & Ness, 2014). However, mechanisms underlying MYB dysregulation and its role in the adaptation of PC cells to a harsh tumor microenvironment are not well defined.

Human antigen R (HuR) is an RNA-binding protein implicated in the post-transcriptional gene regulation (Peng *et al*, 2018). It is overexpressed in PC and other cancers and associated with poor clinical

1 Department of Pathology, College of Medicine, University of South Alabama, Mobile, AL, USA

2 Cancer Biology Program, Mitchell Cancer Institute, University of South Alabama, Mobile, AL, USA

3 Department of Biochemistry and Molecular Biology, College of Medicine, University of South Alabama, Mobile, AL, USA

*Corresponding author. Tel: +1 251 445 9843, Fax: +1 251 460 6994; E-mail: asingh@southalabama.edu

outcomes (Heinonen *et al*, 2005; Wang *et al*, 2013; Peng *et al*, 2018). Here, we present data demonstrating a role for HuR in MYB upregulation, especially under hypoxia, through the stabilization of its transcripts. We also show that MYB acts as a positive regulator of HIF1 α expression and transcriptional activity, and HIF1 α stabilization alone is not sufficient for optimal survival of PC cells under hypoxia. MYB-silenced PC cells fail to metabolically adapt under hypoxia and exhibit downregulation of several genes involved in glucose uptake, glycolysis, and lactate synthesis and transport. MYB binds to and enhances the recruitment of HIF1 α and p300 to the promoter regions of multiple metabolic genes. MYB knockout PC cells exhibit a dramatic reduction in their tumorigenic ability, glucose uptake, and metabolism in an orthotopic mouse model that cannot be rescued by forced overexpression of HIF1 α , supporting an essential role of MYB in PC pathobiology.

Results

MYB expression is crucial for the survival and metabolic reprogramming of pancreatic cancer cells under hypoxia

To investigate the role of MYB in hypoxic survival, three pancreatic cancer cell lines having endogenously high (MiaPaCa and Panc-1) or low (BxPC3) MYB expression were used. MYB expression was silenced in MiaPaCa and Panc-1 cells by stable transfection of MYB-targeting shRNA, whereas it was forcedly overexpressed in BxPC3 cells. Cells were also transfected with scrambled shRNA sequence-expressing plasmid (Scr) or empty vector (Neo) to generate control-paired cell lines (MiaPaCa-Scr/MiaPaCa-shMYB; Panc-1-Scr/Panc-1-shMYB; BxPC3-Neo/BxPC3-MYB). MYB overexpression or knockdown was confirmed intermittently and prior to performing all assays by immunoblotting (Fig EV1A). To examine the effect of MYB modulation on hypoxic survival, cells were cultured under normoxia and hypoxia (1.0% O₂) for different time intervals (0–96 h), and the number of viable cells was counted by trypan blue dye exclusion assay. MYB-silenced cells (MiaPaCa-shMYB and Panc-1-shMYB) exhibited a significant decrease in viable cell number under hypoxia with ~50% reduction by 96 h. In contrast, MYB-overexpressing control cells (MiaPaCa-Scr and Panc-1-Scr) continued to grow and showed a ~30–40% increase in viable cell count in that duration. Similarly, low MYB-expressing BxPC3-Neo cells exhibited ~20% reduced survival under hypoxia, while forced MYB-overexpressing BxPC3-MYB cells had an ~80% increase in their growth after 96 h of incubation under hypoxia (Fig 1A). These findings were further confirmed by flow cytometry-based measurement of Annexin-V and 7-AAD stained cells and fluorescence microscopy analysis of Calcein-AM/EthD-1 staining of live/dead cells. Flow cytometry-based assessment shows a greater proportion of apoptotic cells in MYB knockdown groups than the scrambled control groups, whereas it is decreased in forced MYB-expressing BxPC3-MYB cells relative to low MYB expressing BxPC3-Neo cells (Fig 1B). Similarly, we observe a significant reduction in live: dead cell ratio in MYB-silenced cells cultured under hypoxia for 48 h (Fig EV1B). It is to be noted that MYB silencing and endogenous or forced overexpression sustain for a longer duration upon culturing of the cells under hypoxia (Appendix Fig S1A–C).

Since cancer cells exhibit a metabolic shift towards increased glycolysis and reduced mitochondrial metabolism under hypoxia to

sustain their survival (Guillaumond *et al*, 2013; Eales *et al*, 2016; Lee *et al*, 2020), we examined glucose uptake and lactate secretion in PC cells upon their culturing under hypoxia. We observed a significant increase in glucose uptake and lactate secretion in cells with endogenous or forced MYB-overexpression when cultured under hypoxia. In contrast, MYB-silenced MiaPaCa and Panc-1 cells did not exhibit any significant change, while a modest but significant increase was reported in low MYB-expressing BxPC3 cells (Fig 1C and D). Similarly, we observed that high MYB-expressing control cells exhibited a greater shift towards increased extracellular acidification rate (ECAR) and reduced oxygen consumption rate (OCR) relative to MYB-silenced cells when subjected to hypoxia mimetic condition (Fig 1E and F). To further examine the role of MYB in metabolic reprogramming, we performed metabolite profiling of control and MYB-silenced PC cells cultured under normoxia and hypoxia using high-resolution mass spectrometry (LC-HRMS). As expected, control cells exhibited enhanced glycolytic metabolites under hypoxia with a concomitant decrease in metabolites associated with the TCA cycle. However, MYB-silenced cells exhibited a reduced accumulation of both glycolytic and mitochondrial metabolites under hypoxia (Fig 1G). Interestingly, an increased presence of UDP-glucose and pentose phosphate pathway metabolites were observed in MYB-knockdown cells, whereas high MYB-expressing control cells exhibited increased levels of several amino acids, including serine, tryptophan, asparagine, glycine, and glutamic acid when cultured under hypoxia (Fig 1G). Altogether, these findings suggest that MYB plays an essential role in hypoxic survival by promoting metabolic reprogramming.

MYB expression is induced under hypoxia via a HuR-mediated post-transcriptional mechanism

We next examined the effect of hypoxia on MYB expression in PC cells and observed a time-dependent increase at both protein and mRNA levels (Fig 2A and B). Further, hypoxic induction of MYB was not restricted to PC cells but was also detected in prostate, lung, breast, and colon cancer cell lines (Fig 2C and D). Since HIF1 α is a major hypoxia-responsive transcription factor, we examined if it had a role in MYB induction. MYB expression remained unchanged upon HIF1 α silencing in cells cultured under hypoxia (Fig 2E). Effect of HIF-1 α silencing on its established targets was also examined to confirm its functional inhibition (Fig EV2A). To further confirm this finding, we treated the PC cells with a hypoxia mimetic agent, cobalt chloride (CoCl₂), or prolyl hydroxylases inhibitor, dimethylxaloylglycine (DMOG) that led to hypoxia-independent HIF-1 α stabilization. However, no noticeable change in MYB expression was reported in CoCl₂ or DMOG-treated PC cells (Figs 2F and EV2B). To exclude the possibility of HIF2 α -mediated MYB induction, we silenced its expression prior to the incubation of PC cells under hypoxia. No effect of HIF2 α silencing was observed on MYB induction under hypoxia (Fig EV2C). Moreover, we did not observe any induction of MYB promoter-driven luciferase activity in hypoxia-treated PC cells (Fig 2G), suggesting the possibility of a post-transcriptional regulatory mechanism. Actinomycin D chase assay revealed that MYB mRNA stability was increased significantly under hypoxia ($t_{1/2}$, ~ 4.5 h for MiaPaCa; ~ 4.6 h for Panc-1) relative to that under normoxia ($t_{1/2}$, 2.3 h for MiaPaCa; 2.5 h for Panc-1) (Fig 3A). Furthermore, we also observed

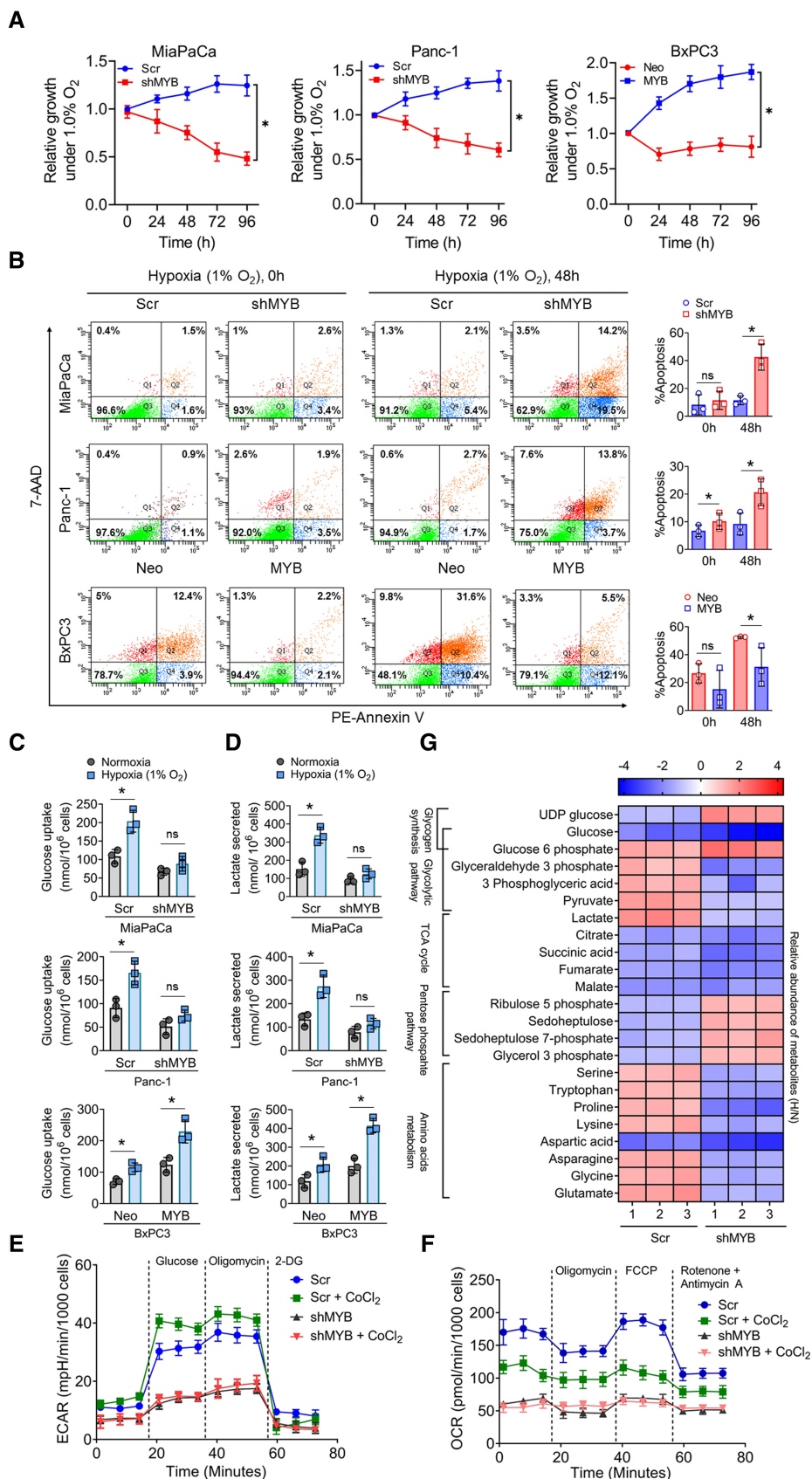


Figure 1.

Figure 1. MYB supports the survival and metabolic adaption of pancreatic cancer cells under hypoxia.

- A MYB knockdown (MiaPaCa-shMYB and Panc1-shMYB) and forced MYB-overexpressing (BxPC3-MYB) PC cells along with their respective control cell lines (MiaPaCa-Scr, Panc1-Scr, and BxPC3-Neo) were subjected to hypoxia (1% O₂) treatment for different time intervals (0–96 h). Their growth was measured by viable cell counting using a trypan blue exclusion assay.
- B Apoptosis indices of genetically engineered MYB-silenced or –overexpressing pancreatic cancer cells were analyzed by flow cytometry after staining with Annexin V and 7-AAD.
- C, D MYB-modulated PC cells were cultured under hypoxia and normoxia for 48 h. Conditioned media was collected and analyzed for consumed glucose (C) and lactate secretion (D). The amount of glucose uptake and lactate secretion was normalized for the number of cells.
- E, F ECAR (E) and OCR (F) in control and MYB silenced MiaPaCa cells cultured under normoxia or treated with hypoxia mimetic CoCl₂ (100 μM for 16 h). Thereafter, ECAR was measured in PC cells with sequential injection of glucose, oligomycin, and 2-DG, while OCR was measured with the serial addition of oligomycin, FCCP, and antimycin A/rotenone.
- G MiaPaCa-Scr and MiaPaCa-shMYB cells were cultured under normoxia and hypoxia for 48 h and harvested for metabolites extraction. The mean area covered by each metabolite's mass spectrum from the triplicate set of LC-HRMS experiments was analyzed and normalized with protein concentration. The heat map was prepared after calculating the relative fold changes of metabolite levels in cells cultured under hypoxia (H) versus normoxia (N).

Data information: Data are shown as means ± SD. The number of technical (A, C–F) and biological (B, G) replicates were 3. The reproducibility of the results (A, C–F) was confirmed at least three times in independent experiments. Two-tailed unpaired Student's *t*-test was used for statistical analyses. n.s., not significant, **P* < 0.05.

greater luciferase activity in PC cells transfected with MYB-3'UTR-luciferase reporter plasmid upon their incubation under hypoxia (Fig EV3A). Therefore, we mapped this region for the putative binding sites of RNA binding proteins (RBPs) using an *in silico* tool (RBPmap). Multiple binding sites for different RBPs, including HuR, were identified in 3'UTR of MYB (Appendix Table S1). HuR-MYB mRNA interaction probability was further established by another *in silico* RNA–protein interaction prediction tool (RPISeq) (Fig EV3B). HuR was of interest since its rapid nuclear to cytoplasmic translocation under hypoxia is reported and associated with mRNA stabilization of genes through binding to the AU-rich elements in their 3'UTRs (Blanco *et al*, 2016; Pan *et al*, 2019). An increase in the cytoplasmic accumulation of HuR in cells cultured under hypoxia was confirmed by immunofluorescence microscopy (Fig 3B) and immunoblot analyses (Fig 3C). Increased cytoplasmic accumulation of HuR under hypoxia was independent of HIF1α or HIF2α (Fig EV3C and D). Subsequently, we validated the interaction of MYB 3'UTR with HuR by RNA-IP assay in cells cultured under hypoxia (Figs 3D and EV3E) and determined the effect of HuR silencing on MYB expression. HuR silencing reduced the luciferase activity in a MYB-3'UTR-reporter assay (Fig 3E) and decreased the half-life of MYB mRNA under both normoxia (siCtrl, ~ 2.4 h; siHuR, 1.9 h) and hypoxia (siCtrl, ~ 4.6 h; siHuR, ~ 2.6 h) (Fig 3F). Also, we observed decreased levels of MYB mRNA and protein in HuR-silenced PC cells (Fig 3G).

MYB binds to the HIF1α promoter and transcriptionally upregulates its expression

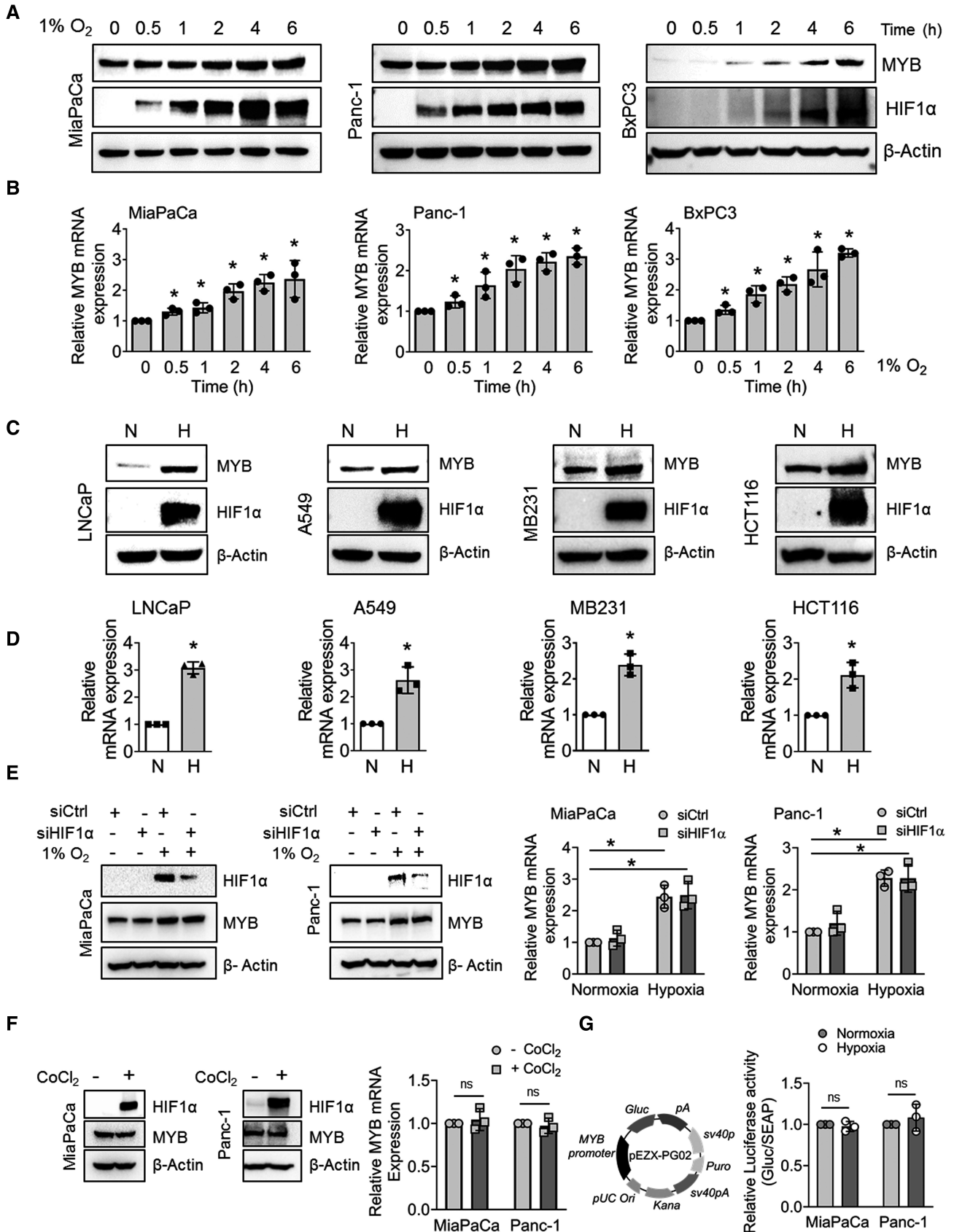
HIF1α is a master regulator of hypoxia adaptive response, which gets rapidly stabilized under hypoxia due to the inhibition of its proteasomal degradation (Salceda & Caro, 1997). Having observed a role of MYB in hypoxic survival, we examined if it had any effect on HIF1α expression. Immunoblot analysis demonstrated that after incubation in hypoxia, high MYB-expressing control cells accumulated greater levels of HIF1α compared with the MYB-silenced cells or those having low endogenous MYB expression (Fig 4A). Interestingly, we also observed higher levels of HIF1α transcript in MYB-overexpressing cells under both hypoxic and normoxic conditions (Fig 4B). A significant reduction in the transcriptional activity of the HIF1α promoter was also reported in MYB-silenced PC cells under both normoxia (~ 1.9 folds, MiaPaCa; ~ 2.0 folds, Panc-1) and hypoxia (~ 3.0 folds, MiaPaCa; ~ 2.8 folds, Panc-1). Likewise, forced overexpression of MYB in BxPC3 enhanced the HIF1α promoter activity under both normoxia (~ 2.9 folds) and hypoxia (~ 3.5 folds) (Fig 4C). No MYB-dependent changes in HIF1α mRNA stability were reported in either MYB-silenced or MYB-overexpressing PC cells (Appendix Fig S2). We next examined the possibility of MYB-mediated direct transcriptional regulation of HIF1α. *In silico* analysis using PROMO-ALGGEN (Messeguer *et al*, 2002) and TFBIND (Tsunoda & Takagi, 1999) identified three putative MYB

Figure 2. MYB upregulation under hypoxia is HIF1α-independent and does not occur at the transcriptional level.

- A MYB expression was analyzed by immunoblotting in pancreatic cancer cells cultured under hypoxia for different time intervals. HIF1α accumulation was examined as a positive control.
- B MYB transcript levels were determined by qRT-PCR in hypoxia-treated cells.
- C, D MYB protein (C) and transcript (D) levels were measured in the prostate (LNCaP), lung (A549), breast (MB231), and colon (HCT116) cancer cells cultured under normoxia and hypoxia (6 h) by immunoblotting and qRT-PCR, respectively. β-Actin/ACTB served as an internal control. N- normoxia and H- hypoxia.
- E Pancreatic cancer cells were transiently transfected either with non-targeted control siRNA (siCtrl) or HIF1α-targeting siRNA (siHIF1α) for 24 h and then incubated under hypoxia for 6 h. MYB expression was analyzed at protein and mRNA levels.
- F Cells were treated with either vehicle or CoCl₂ (100 μM) for 6 h, and total protein and RNA were isolated. The expression of HIF1α and MYB was examined. β-Actin was used as an internal control.
- G Cells were co-transfected with a plasmid expressing Gaussia luciferase under the control of MYB promoter and secreted alkaline phosphatase (SEAP) expression plasmid under a constitutive CMV promoter. After 24 h, media was replaced and cells were cultured under normoxia or hypoxia for 6 h. Luciferase and SEAP activities were analyzed and data presented as relative luciferase activity normalized with SEAP activity.

Data information: Data are shown as means ± SD. The number of technical (B, D–G) replicates was 3. Reproducibility of the results (A–G) was confirmed at least three times in independent experiments. Two-tailed unpaired Student's *t*-test was used for statistical analyses. n.s., not significant, **P* < 0.05.

Source data are available online for this figure.



binding regions upstream of the transcription start site in the HIF1 α promoter (Fig 4D), of which significant enrichment of MYB was recorded in the proximal region under both normoxia and hypoxia by chromatin immunoprecipitation (ChIP) assay (Fig 4E). Together, these findings suggest that MYB transcriptionally upregulates HIF1 α by directly binding to its promoter.

HIF1 α overexpression in MYB-silenced pancreatic cancer cells fails to rescue their survival and metabolic adaptation under hypoxia

Having observed reduced HIF1 α accumulation in MYB-silenced PC cells, we next examined whether restoring HIF1 α expression would

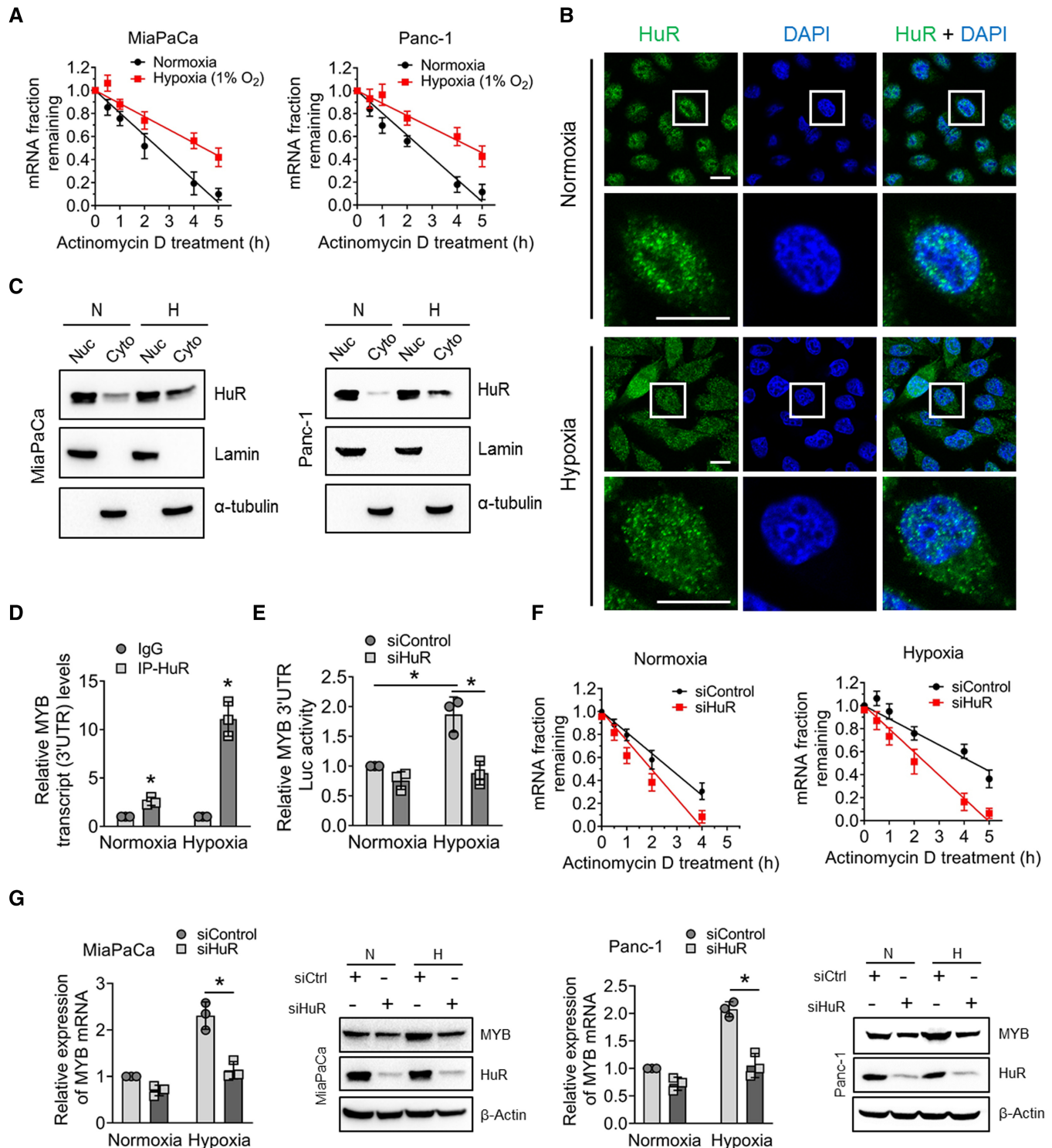


Figure 3.

Figure 3. MYB is induced under hypoxia via a HuR-mediated post-transcriptional mechanism.

- A Cells were pre-treated with Actinomycin D (10 μ g/ml) for 1 h followed by incubation under normoxia or hypoxia for indicated time points. Total RNA was collected and MYB mRNA levels were examined by q-RT PCR. 18s rRNA was used as an internal control.
- B HuR localization was examined by immunofluorescence microscopy in cells exposed to hypoxia for 1 h. HuR (green), and nucleus (blue). Scale bar, 25 μ m (lower left corner). Lower panels are digitally magnified views of the marked rectangles.
- C Cytosolic and nuclear protein fractions were prepared from cells cultured under hypoxia for 1 h and HuR expression was examined by immunoblotting. α -Tubulin (nuclear) and Lamin A (cytoplasm) were used as loading controls.
- D RNP-IP assay was performed using the cytoplasmic fractions of cells exposed to hypoxia for 3 h. Following DNase I treatment, cytoplasmic fractions were sonicated and subjected to immunoprecipitation using an anti-HuR antibody. MYB mRNA was checked by qRT-PCR from isolated RNA fragments and normalized with IgG isotype control. 18s rRNA was used as an internal control.
- E Following transfection with siHuR or control siRNA for 24 h, cells were co-transfected with MYB 3'-UTR-firefly luciferase reporter and Renilla luciferase-expressing control plasmid. After 24 h, cells were incubated under hypoxia for 6 h. Data are presented as Firefly luciferase activity normalized with Renilla luciferase activity.
- F Cells transfected with HuR or control siRNA for 48 h were pretreated with Actinomycin D (10 μ g/ml) for 1 h and then cultured under normoxia and hypoxia for various time points (0–6 h). Total RNA was collected, and MYB mRNA levels were checked in HuR-silenced cells by q-RT PCR. 18s rRNA was used as an internal control.
- G Cells transfected with HuR or control siRNA for 48 h were exposed to hypoxia for 6 h, and MYB and HuR expression was determined by immunoblotting or qRT-PCR.

Data information: Data are shown as means \pm SD. The number of technical (A, D–G) replicates was 3. Reproducibility of the results (A–G) was confirmed at least three times in independent experiments. Two-tailed unpaired Student's *t*-test was used for statistical analyses. **P* < 0.05. Source data are available online for this figure.

rescue their growth under hypoxia. For this, we forcedly overexpressed HIF1 α under the control of a constitutive CMV promoter in MYB knockdown PC cells (Fig 5A). After that, we cultured these cells under hypoxia for different time duration and examined their growth using the trypan blue dye exclusion assay. Our results show that despite restored expression of HIF1 α , MYB-silenced PC cells exhibited a \sim 35% decrease in their growth when cultured under hypoxia for 96 h, whereas \sim 25–30% increase was reported in both MYB and HIF1 α -expressing PC cells in that duration (Fig 5B). These observations were further confirmed by live-dead cell staining, which showed that MYB-silenced PC cells continued to exhibit increased proportion of dead cells under hypoxia even after restored HIF1 α expression (Fig 5C). Notably, when we performed metabolic profiling of MYB-silenced cells after exogenously restoring HIF1 α expression, we still did not see a desired metabolic shift (Fig 5D and E). These findings were further confirmed by glucose uptake and lactate secretion assays (Fig 5F). Interestingly, in a converse approach, we found that HIF1 α silencing in ectopic MYB-overexpressing cells diminished their survival, glucose uptake, and lactate secretion, thus underscoring the functional significance of MYB-HIF1 α crosstalk in hypoxia adaptive responses (Fig EV4A–E).

MYB regulates the expression of metabolic genes and facilitates the recruitment of HIF1 α and p300 to their promoters under hypoxia

HIF1 α is a crucial regulator of transcriptional reprogramming under hypoxia that helps cancer cells in the metabolic adaptation (Majmudar *et al.*, 2010; Eales *et al.*, 2016). Since we observed that MYB-silenced PC cells failed to adapt metabolically under hypoxia despite exogenous HIF1 α overexpression, we explored the role of MYB in transcriptional response to hypoxia. For this, we examined the expression profile of a panel of adaptive metabolism response-associated genes in MYB-overexpressing and knockdown PC cells under normoxia and hypoxia. The data reveal that MYB silencing affected the ability of PC cells to make adaptive changes in the expression of several genes involved in glucose transport, glycolysis, gluconeogenesis, pentose phosphate pathway, and lactate transport under hypoxia (Fig 6A). This adaptive transcriptional response was not rescued for several genes even after the restoration of HIF1 α

expression, even though many of them are established HIF1 α targets (Fig 6B), leading us to hypothesize that MYB and HIF1 α engage in cooperative gene regulation. Therefore, we performed *in silico* analysis and identified putative MYB binding sites in the promoter of at least five genes (*GLUT3*, *HK2*, *PFKL*, *ENO2*, and *MCT4*) in close vicinity of hypoxia response elements (HRE) (Appendix Fig S3A–E). ChIP analyses showed that MYB was efficiently bound to the proximal promoter regions of *HK2*, *ENO2*, and *MCT4* and the distal region of *GLUT3* and *PFKL* promoters, and MYB binding was further increased under hypoxia (Fig 6C). Subsequently, we analyzed the effect of MYB on HIF1 α binding to the HRE in these gene promoters under hypoxia and found that HIF1 α binding was significantly reduced in MYB-silenced cells and only partly rescued in MYB-silenced, HIF1 α -overexpressing cells (Fig 6D). Moreover, our data from ChIP assays demonstrated enhanced p300 binding on the promoters of metabolic genes under hypoxia and enhanced histone H3 acetylation at lysine9 (H3K9-Ac) in MYB-expressing cells relative to MYB-silenced cells (Fig 6E and F). Furthermore, MYB co-immunoprecipitated with HIF1 α and its co-activator, p300 (Fig 7A and B), and exhibited nuclear co-localization (Fig 7C and D).

MYB knockout pancreatic cancer cells exhibit reduced tumorigenicity, glucose uptake, and lactate synthesis *in vivo* despite restored HIF1 α expression

Next, we sought to determine the significance of our observations in an orthotopic mouse model. We first generated the MYB knockout (MYB KO) MiaPaCa cell line using CRISPR-Cas9 technology (Appendix Fig S4A and B) to avoid any artifact emerging from the clonal selection in the long-term animal study. After that, HIF1 α was stably overexpressed in MYB KO cells (Appendix Fig S4C). The luciferase-tagged control, MYB KO and MYB KO- HIF1 α ^{OE} cells were injected into the mouse pancreas, and growth was monitored weekly by *in vivo* imaging (Fig 8A). Mice were sacrificed after 5 weeks, and data were recorded for tumor size and weight. The data show that MYB KO cells had drastically reduced tumor growth, which could not be rescued after ectopic HIF1 α overexpression (Fig 8B and C). Further, analysis of tumor xenografts showed reduced levels of glucose (Fig 8D), lactate (Fig 8E), and citrate (Fig 8F) in both MYB KO and MYB KO-HIF1 α ^{OE} cells. Pimonidazole (PDZ) adduct staining

demonstrated more number of hypoxic foci in control tumor xenografts, compared with MYB KO and MYB KO-HIF1 α^{OE} xenografts (Fig EV5A–C). Furthermore, examination of serial sections stained for MYB, MCT4, GLUT3, and HK2 within the PDZ-positive areas

showed their decreased expression in MYB KO and MYB KO-HIF1 α^{OE} tumors, compared with the control group (Fig 8G). Altogether, our findings demonstrate *in vivo* significance of MYB in pancreatic tumorigenicity and metabolic reprogramming.

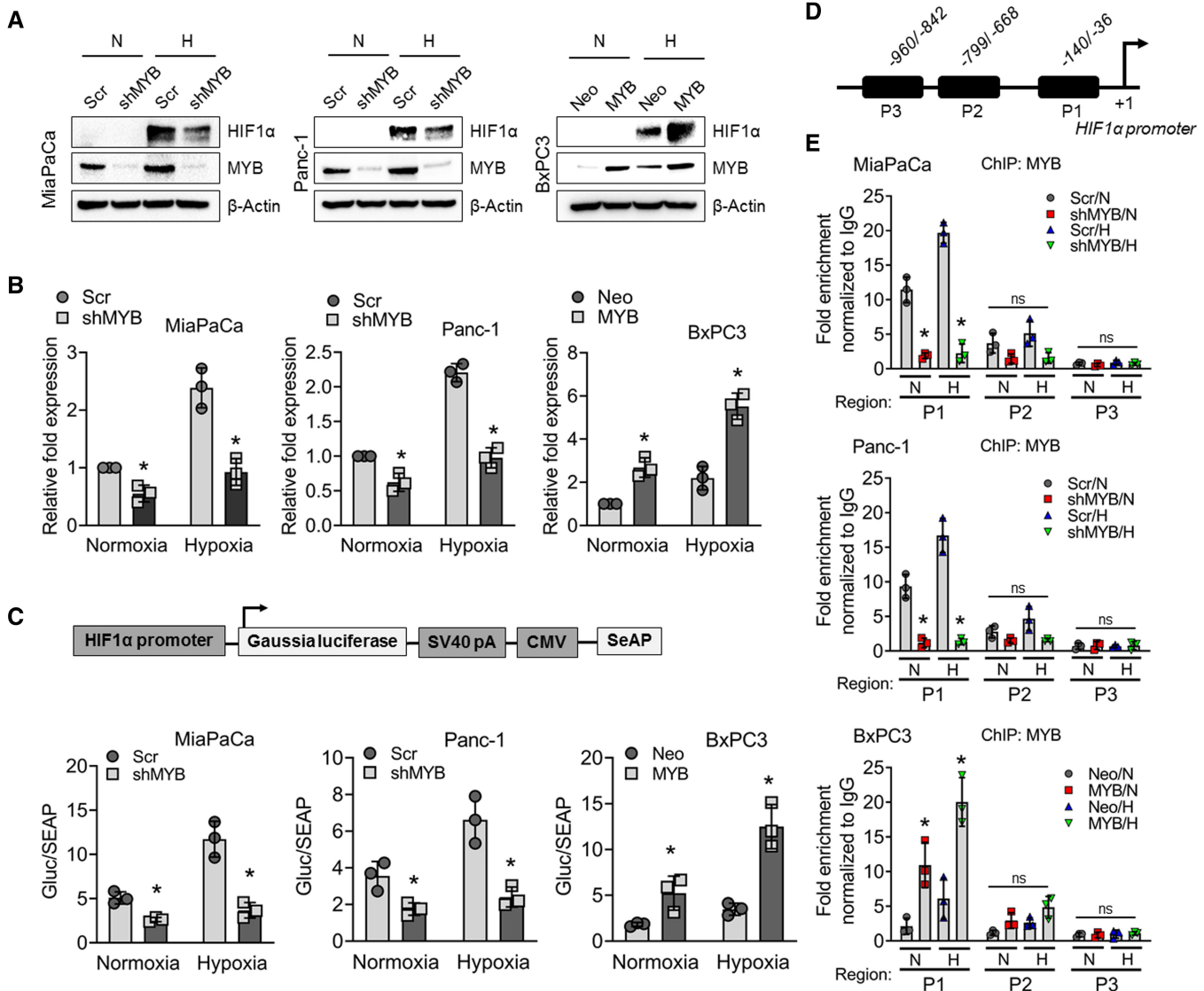


Figure 4. MYB regulates HIF1 α expression at the transcriptional level by directly binding to its promoter.

- A** MYB-silenced (MiaPaCa-shMYB and Panc1-shMYB) and MYB-overexpressing (BxPC3-MYB) PC cells, along with their control cell lines (MiaPaCa-Scr, Panc1-Scr, and BxPC3-Neo) were exposed to hypoxia for 6 h. Protein lysates were made, and the expression of MYB and HIF1 α was examined by immunoblotting. β -Actin served as a loading control.
- B** Total RNA was also isolated from MYB-modulated pancreatic cancer cells incubated under hypoxia (6 h). Levels of HIF1 α transcripts were measured by qRT-PCR. β -Actin served as an internal control. Bars represent relative fold change in HIF1 α transcripts.
- C** The transcriptional activity of the HIF1 α promoter was determined by performing the promoter-reporter assay. MYB-modulated PC cell lines were transfected with the reporter plasmid, and after 24 h of transfection, cells were cultured under hypoxia or normoxia for 24 h, and the supernatant was collected. HIF1 α promoter-driven Gussia luciferase activity was normalized with SEAP activity, and the data were presented as a bar diagram.
- D** *In silico* analysis of the HIF1 α promoter was performed to identify MYB binding sites using PROMO- ALGGEN and TFBIND. Three putative binding regions, P1 (–36 to –140), P2 (–668 to –799), and P3 (–842 to –960) preceding the transcription start site, were predicted.
- E** MYB-silenced or -overexpressing PC cell lines were exposed to normoxia or hypoxia for 6 h and subjected to chromatin immunoprecipitation using anti-MYB antibodies or IgG control followed by qPCR analysis using site-specific primers.

Data information: Data are shown as means \pm SD. The number of technical (B, C, E) replicates was 3. The reproducibility of the results (A–C, E) was confirmed at least three times in independent experiments. Two-tailed unpaired Student's *t*-test was used for statistical analyses. n.s., not significant, **P* < 0.05.

Source data are available online for this figure.

Discussion

Pancreatic cancer (PC) is characterized by poor tumor vasculature and high desmoplasia, making it one of the most hypoxic malignancies. Yet pancreatic tumor cells not only acclimatize to such a harsh hypoxic microenvironment but also exhibit relentless, aggressive progression due to their evolved adaptive properties. The current

study identified MYB as an essential mediator of the hypoxic survival and hypoxia-induced metabolic adaptation of PC cells. We observed that MYB expression increased under hypoxia via HuR-mediated stabilization of its mRNA. Further, MYB transcriptionally upregulated HIF1 α by binding to its promoter and acted in cooperation to regulate the expression of metabolic genes. We also observed that in the absence of MYB, HIF1 α was not able to confer hypoxic

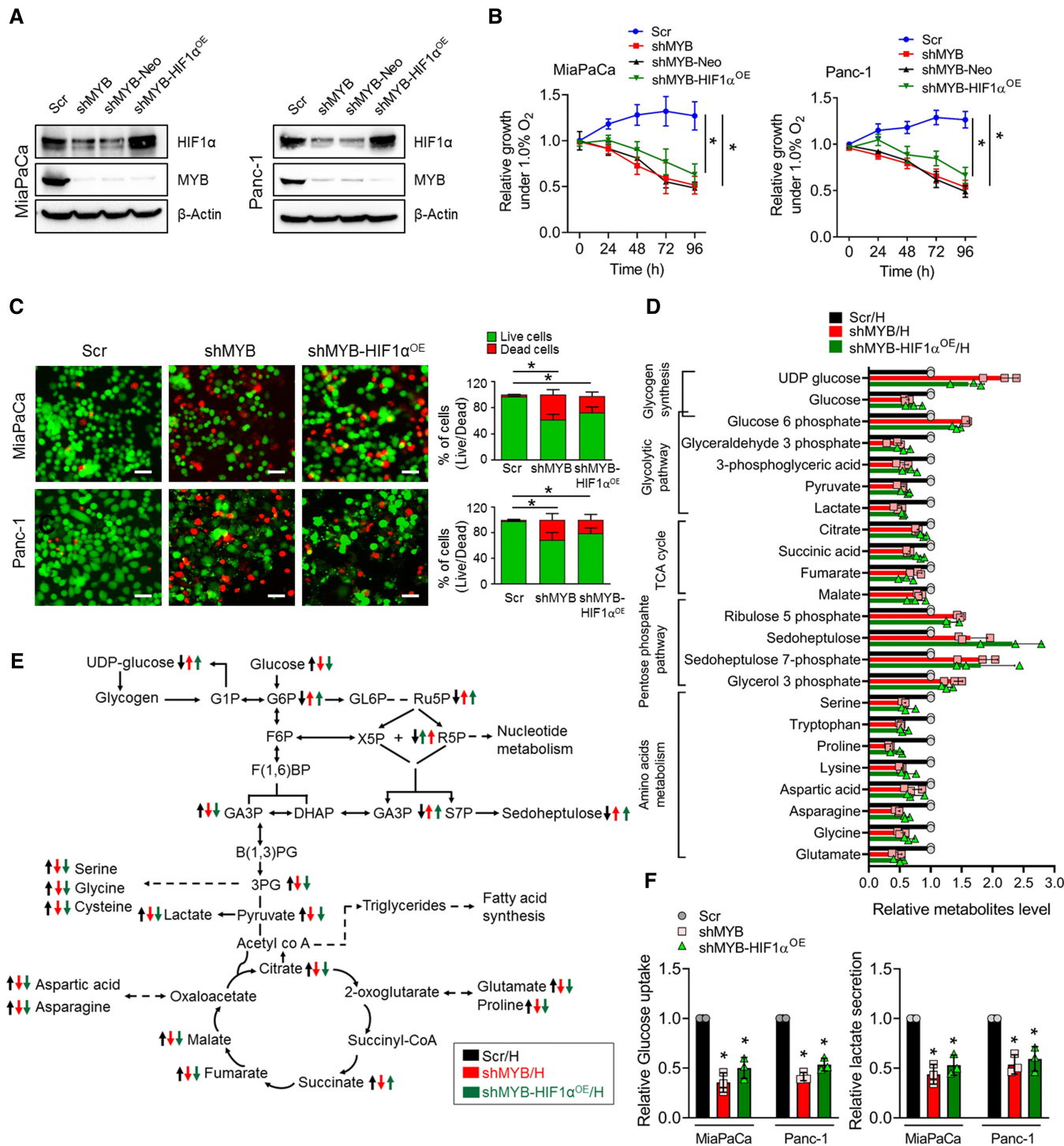


Figure 5.

Figure 5. Forced expression of HIF1 α in MYB-silenced pancreatic cancer cells fails to rescue their survival and metabolic shift under hypoxia.

- A Immunoblot analysis was performed to analyze HIF1 α and MYB expression in MYB-silenced (shMYB) and those having a forced overexpression of HIF1 α (shMYB-HIF1 α ^{OE}) along with their respective controls (Scr and shMYB-Neo) cultured under hypoxia. β -Actin served as a loading control.
- B The cell viability was determined by trypan blue exclusion method in MYB knockdown cells or with ectopic expression of HIF1 α in MiaPaCa and Panc-1 along with their control cells exposed to hypoxia at different time intervals (0–96 h).
- C Live/Dead staining was performed in MYB-silenced MiaPaCa and Panc-1 or MYB silenced- HIF1 α overexpressed cells cultured under hypoxia for 48 h. Cells were visualized under a fluorescence microscope. Representative fluorescence micrographs are presented. The number of live and dead cells was counted from the captured random images. Scale bar, 150 μ m (lower right corner).
- D Relative levels of metabolites were calculated in MiaPaCa-Scr, -shMYB, and -HIF1 α -overexpressing shMYB cells exposed to hypoxia, and data normalized with protein concentration.
- E A schematic diagram shows metabolic pathways with altered changes in metabolites in genetically engineered cell lines having a differential expression of MYB and HIF1 α .
- F MYB-silenced and HIF1 α overexpressing MYB knockdown PC cells and control cells were cultured under hypoxia for 48 h. Conditioned media was collected and analyzed to assess glucose consumption and lactate secretion by measuring their levels. The data were normalized with the number of cells and presented as relative fold changes.

Data information: Data are shown as means \pm SD. The number of technical (B–D, F) replicates was 3. The reproducibility of the results (A–D, F) was confirmed at least three times in independent experiments. Two-tailed unpaired Student's *t*-test (B, F) and one-way ANOVA (C) were used for statistical analyses. **P* < 0.05.

Source data are available online for this figure.

cell survival as it failed to sufficiently cause desired alterations in metabolic gene regulation and cellular metabolism. We found that MYB bound to the promoters of several critical metabolic genes and facilitated HIF1 α recruitment by causing histone modifications. Consequently, a significant reduction in the tumorigenicity of pancreatic cancer cells was also observed that could not be regained even after forced overexpression of HIF1 α . These findings add a new mechanistic dimension to our previous observations suggesting a role of MYB in the pancreatic tumor pathobiology (Srivastava *et al*, 2015; Azim *et al*, 2016; Bhardwaj *et al*, 2016; Zubair *et al*, 2020).

The hypoxic microenvironment profoundly impacts the molecular and biological properties of cancer cells (Choudhry & Harris, 2018; Petrova *et al*, 2018; Lee *et al*, 2020). These changes are predominantly mediated through HIF1 α , which mediates the adaptive changes in the gene expression (Dengler *et al*, 2014; Wang *et al*, 2021). However, in our findings, we did not see an effect of HIF1 α silencing or accumulation on MYB expression. Instead, we identified that MYB was regulated post-transcriptionally via HuR, resulting from its enhanced cytoplasmic accumulation and enhanced binding to 3'UTR of MYB transcript under hypoxia. HuR has previously been shown to exhibit cytoplasmic translocation under hypoxic conditions and post-transcriptionally regulate the expression of other genes (Blanco *et al*, 2016; Reglero *et al*, 2020). In other reports, post-transcriptional regulation of MYB via miRNA or other mechanisms has been demonstrated (Gudas *et al*, 1995; Xiao *et al*, 2007; Navarro *et al*, 2009; Mets *et al*, 2015; Elcheva *et al*, 2020). However, our findings are the first to show hypoxia-

induced MYB upregulation involving a HuR-mediated mechanism. Overexpression of HuR has been reported in pancreatic and other gastrointestinal cancers and is associated with aggressive tumor phenotypes and chemoresistance (Mrena *et al*, 2005; Costantino *et al*, 2009). In that context, our findings identify a novel HuR-MYB axis that supports the hypoxia survival of pancreatic cancer cells.

Post-translational ubiquitination following oxygen-dependent hydroxylation on proline residues (P402 and P564) by prolyl hydroxylases (PHDs) is considered a significant mechanism for HIF1 α regulation. Under hypoxia, the activity of PHDs is inhibited due to decreased oxidation preventing ubiquitin-mediated HIF1 α proteasomal degradation (Salceda & Caro, 1997; Semenza, 2013; Choudhry & Harris, 2018). However, some reports indicate HIF1 α regulation by oxygen-independent mechanisms. It is shown that other post-translational mechanisms, such as methylation and acetylation, can enhance HIF1 α stability primarily in the nucleus, independent of proline hydroxylation, under both normoxic and hypoxic conditions (Kim *et al*, 2016). On the contrary, a hypoxia-inducible miRNA, miR-429, is shown to cause post-transcriptional repression of HIF1 α , while in other reports, NF- κ B is shown to act as its transcriptional regulator (Arora *et al*, 2013; Azoitei *et al*, 2016). Thus, our findings demonstrating transcriptional regulation of HIF1 α by MYB under both normoxia and hypoxia suggest another novel mode of HIF-1 α regulation in pancreatic cancer.

Cancer cells undergo metabolic reprogramming to support their survival and proliferation under a hypoxic environment. These changes include a shift from mitochondrial oxidative phosphorylation

Figure 6. MYB alters the expression of a select set of metabolic genes by binding to their promoters and enhancing the recruitment of HIF1 α and p300.

- A MYB modulated PC cells (MiaPaCa Scr and shMYB) were cultured under normoxia/hypoxia for 12 h. Afterward, total RNA was isolated, and relative fold change in the mRNA expression of genes associated with glucose metabolism was examined by qRT-PCR. *ACTB* was used as an internal control.
- B Heat map showing the relative fold changes in glucose metabolism-associated gene expression in Scr control, shMYB, and shMYB-HIF1 α ^{OE} MiaPaCa and Panc-1 cells cultured under hypoxia for 12 h.
- C Quantitative ChIP-qPCR was performed to analyze the occupancy of MYB under normoxia and hypoxia at promoter regions of selected glycolytic genes (*GLUT3*, *HK2*, *PFKL*, *ENO2*, and *MCT4*) using anti-MYB or IgG control antibodies. The enrichment of promoter regions was compared between cells cultured under normoxia or hypoxia.
- D–F Genomic occupancy of HIF1 α (D), p300 (E), and H3K9ac (F) on the promoter regions were also confirmed by ChIP-qPCR using specific antibodies and fold enrichment calculated and presented as a bar graph after normalization with control IgG.

Data information: Data are shown as means \pm SD. The number of technical (A–F) replicates was 3. The reproducibility of the results (A–F) was confirmed at least three times in independent experiments. Two-tailed unpaired Student's *t*-test was used for statistical analyses. **P* < 0.05.

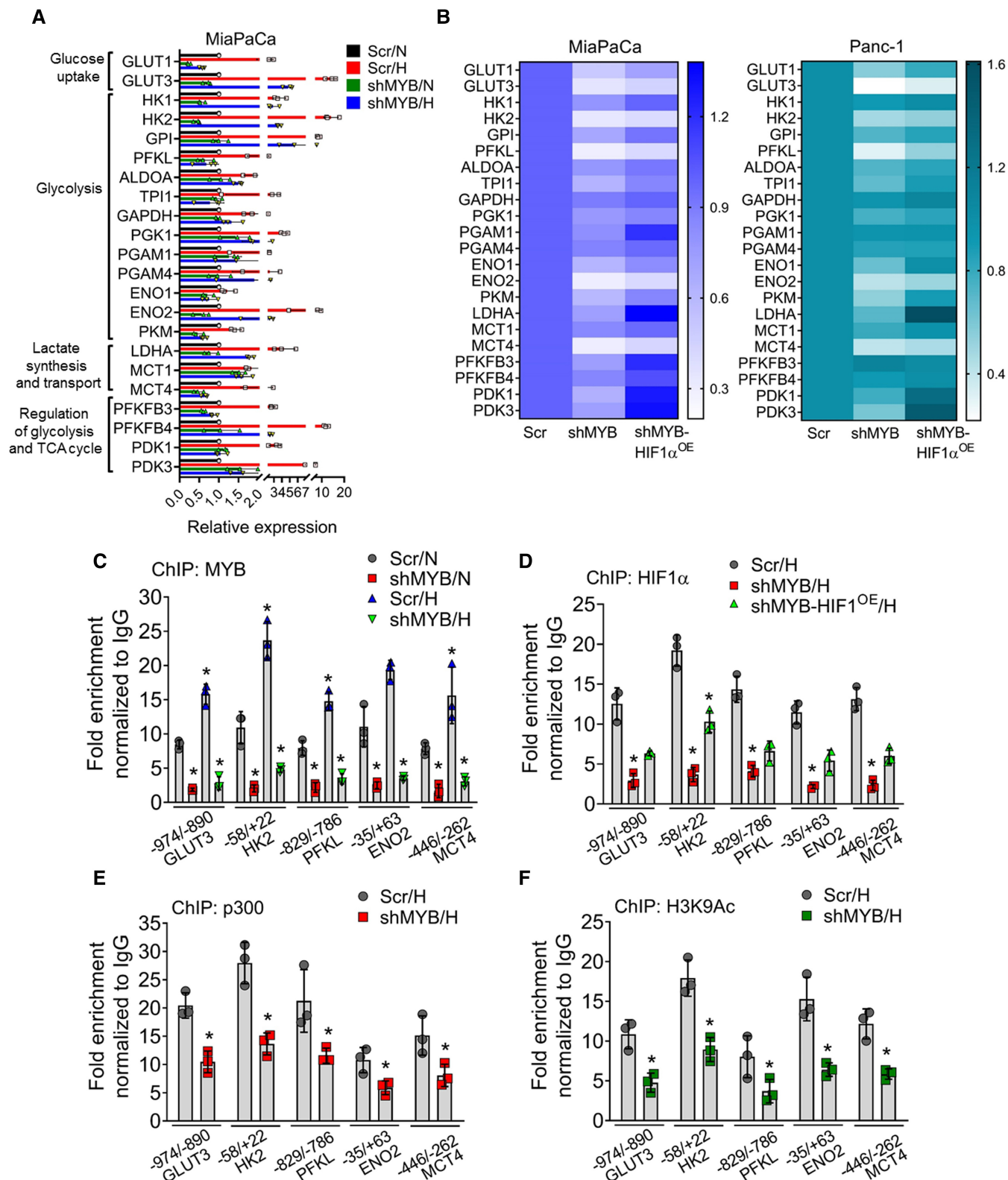


Figure 6.

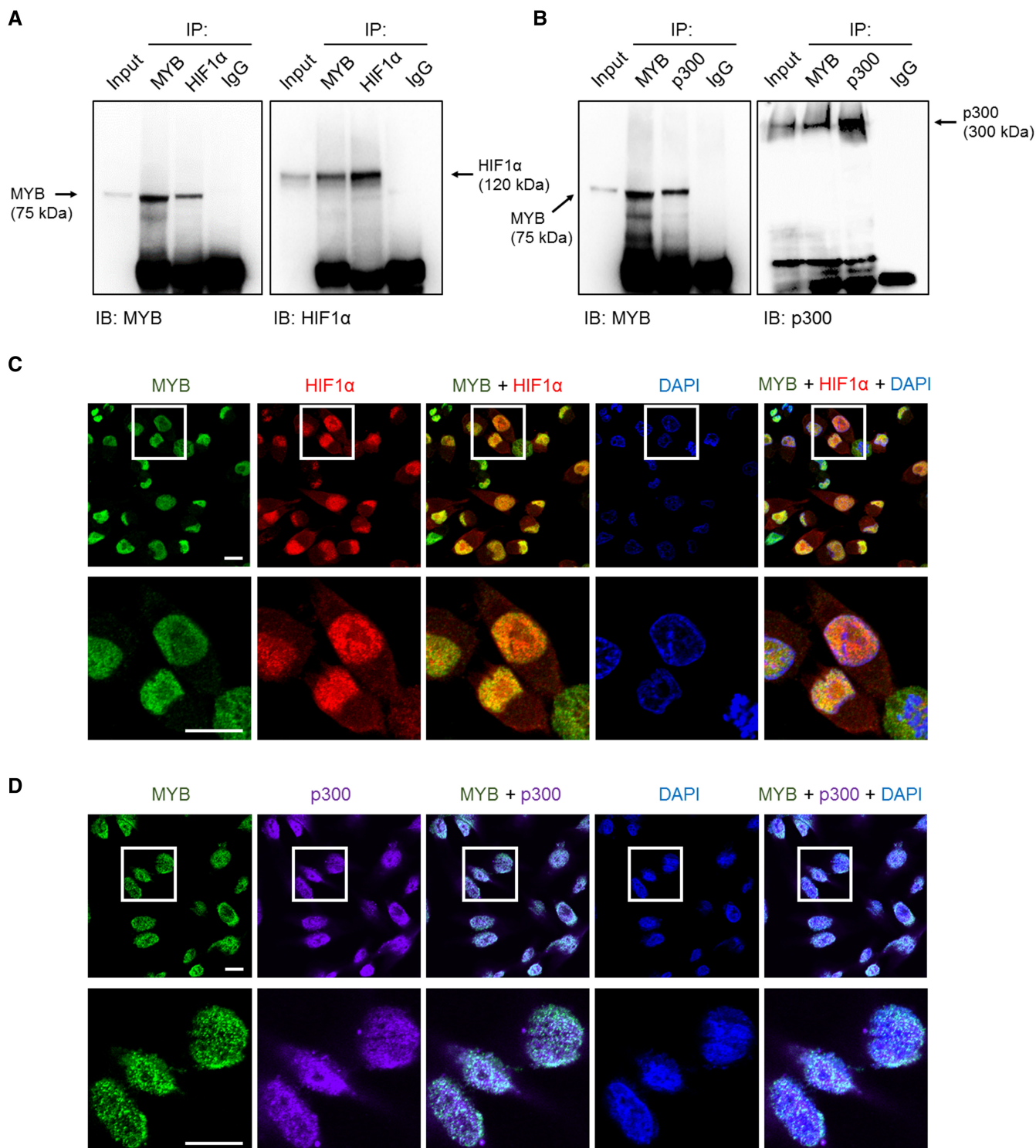


Figure 7. MYB interacts with HIF1 α and p300 and exhibits nuclear co-localization.

A, B Interaction of MYB with HIF1 α (A) and p300 (B) was examined by co-immunoprecipitation assays in the lysates of pancreatic cancer cells cultured under hypoxia for 6 h. Immunoprecipitation with IgG isotype antibody was used as a control. 10% of total cell lysate was used as input for western blot analysis.

C, D Co-localization of MYB with HIF1 α (C) and p300 (D) was examined in pancreatic cancer cells grown under hypoxia for 6 h by immunofluorescence assays followed by confocal microscopy. Scale bar, 30 μ m (lower left corner). Lower panels are digitally magnified views of the marked rectangles. For ease of visualization, a pseudo color (purple) was adopted for p300 staining.

Data information: Reproducibility of the results (A–D) was confirmed at least three times in independent experiments.

Source data are available online for this figure.

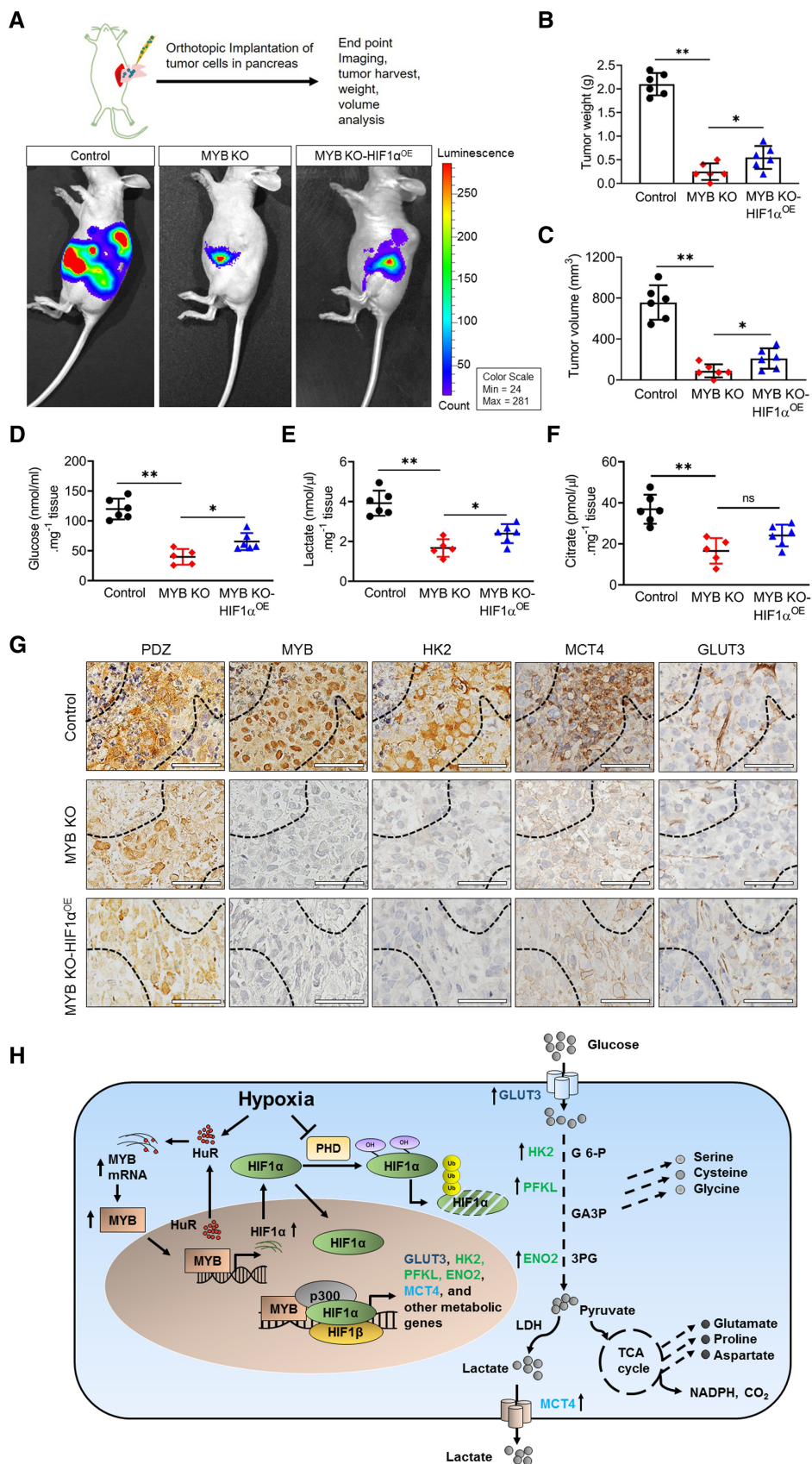


Figure 8.

Figure 8. Tumorigenicity of MYB-silenced PC cells remains significantly reduced despite restored HIF1 α expression.

- A Luciferase tagged-MiaPaCa control, MYB knockout, or HIF1 α overexpressed MYB knockout cells were implanted into the tail of the pancreas of athymic nude mice ($n = 6$ per group).
- B, C Tumor growth was monitored by non-invasive bioluminescence imaging. Tumors were resected at the experimental endpoint, and their weights (B) and volumes (C) were recorded.
- D–F The levels of glucose (D), lactate (E), and citrate (F) were also analyzed in the tumor tissues and normalized with the tissue weight used for metabolite extraction.
- G Tumor xenograft serial sections were immunostained for pimonidazole (PDZ) adduct, MYB, HK2, GLUT3, and MCT4 using specific antibodies. Images were taken at 40 \times magnification. Scale bar, 60 μ m (lower left corner). The dashed lines demarcate the hypoxic region based on the PDZ staining pattern.
- H Schematic figure showing MYB expression is induced under hypoxia via HuR, which then transcriptionally upregulates HIF1 α leading to its more significant accumulation under hypoxia. Further, MYB interacts with HIF1 α and p300 and enhances their recruitment to glycolytic gene promoters. Transcriptional upregulation of glycolytic genes via coordinated action of MYB, HIF1 α , and p300 helps in the metabolic adaptation of cancer cells to sustain their growth and survival.

Data information: Data are shown as means \pm SD ($n = 6$). The number of technical (D–F) replicates was 3. A one-way ANOVA test was used for statistical analyses. * $P < 0.05$, ** $P < 0.01$.

to cytoplasmic glycolysis because of decreased oxygen availability, and HIF1 α is suggested to be a primary driver of these metabolic alterations (Denko, 2008; Semenza, 2013; Eales *et al*, 2016). However, in our study, MYB-silenced pancreatic cancer cells failed to survive and exhibit the desired change in cellular metabolism despite forced overexpression of HIF1 α . Indeed, we found that the knockdown of MYB greatly affected the glucose and amino acid metabolism in pancreatic cancer cells, even under well-oxygenated conditions. A significant decrease was recorded in intracellular glucose, pyruvate, and glycolytic and TCA cycle intermediates under both normoxia and hypoxia in MYB knockdown cells. Interestingly, we observed increased levels of UDP-glucose and glucose 6-phosphate in MYB knockdown cells, which is indicative of the conversion of glucose to glycogen. It is shown that glycogen content in the cells inversely correlates with the proliferation rate (Rousset *et al*, 1981). Further, hypoxia induces an early glycogen accumulation followed by a gradual decline as cells adapt and regain their proliferation (Favaro *et al*, 2012). Thus, the continued shift towards glycogen synthesis in MYB knockdown cells may suggest their impaired ability to adapt under hypoxia. Moreover, increased levels of pentose phosphate pathway intermediates in MYB knockdown cells could indicate a metabolic shift due to the underutilization of glucose 6-phosphate via glycolytic and TCA cycle pathways (Jiang *et al*, 2014). Besides glucose metabolism, we observed a noticeable decrease in the accumulation of several amino acids in MYB knockdown cells, exhibiting further reduction under hypoxia. This could be due to their reduced uptake or decreased availability of glycolytic and TCA cycle intermediates, limiting their shunting into the amino acid biosynthetic pathways (Jochmanova & Pacak, 2016; Xu *et al*, 2020).

Since MYB-silenced pancreatic cancer cells failed to adapt metabolically despite the restored expression of HIF1 α , we examined its effect on the hypoxia-induced transcriptional response on crucial metabolic genes. The data revealed that MYB downregulation affected the ability of pancreatic cancer cells to upregulate the expression of several genes, including those involved in glucose uptake (*GLUT3*), glycolysis (*HK2*, *PFKL*, and *ENO2*), and lactate transport (*MCT4*). Furthermore, we confirmed that MYB physically bound and occupied the promoter region of these genes, and its binding increased under hypoxia. We also observed that MYB enhanced the recruitment of HIF1 α and histone acetyltransferase p300 to the promoter of these genes and increased the H3K9 acetylation and HIF1 α transcriptional activity. Thus, our findings suggest that MYB modulates hypoxia signaling by not only regulating the

levels of HIF1 α but also supporting its interaction with its target gene promoters. It is reported that p300 acts as a coactivator for both MYB and HIF1 α and enhances their transcriptional activity through the chromatin modification (Arany *et al*, 1996; Kasper *et al*, 2002; Liu *et al*, 2015; Fuglerud *et al*, 2018). By co-immunoprecipitation and confocal microscopy, we confirmed the interaction of MYB with both HIF1 α and p300, indicating their presence in a transcriptional complex that facilitates hypoxia-induced transcriptional reprogramming. A large body of evidence suggests MYB and HIF1 α interaction with other transcription factors (Pawlus *et al*, 2014; Srivastava *et al*, 2021). Indeed, a recent genome-wide ChIP-seq analysis of human acute myeloid leukemia cells has identified MYB binding sites in the vicinity of HIF1 α bound regions in gene promoters, along with other transcription factors suggestive of their cooperative action in the gene regulation (Wierenga *et al*, 2019).

In summary, our findings support a crucial role of MYB in the hypoxic survival of pancreatic cancer cells (Fig 8H). We identify MYB as a novel transcriptional regulator of HIF1 α expression and present evidence for a novel mechanistic relationship between these two proteins. We show that MYB interacts with HIF1 α and p300 and enhances their occupancy on glycolytic gene promoters through chromatin modification. An impact of MYB on cellular metabolism regardless of oxygen availability is suggestive of its both HIF1 α -dependent and -independent functions. It appears that MYB is essential for the metabolic plasticity of the cancer cell and helps it adapt to the constantly changing surrounding environment.

Materials and Methods

Cell lines, transfection, and treatment

Human pancreatic cancer (PC) cell lines, MiaPaCa (high MYB-expressing), Panc1 (high MYB-expressing), and BxPC3 (low MYB-expressing), were used in this study. Their stable knockdown (MiaPaCa-shMYB and Panc-1-shMYB) and forced overexpressing (BxPC3-MYB) derivative lines along with corresponding control cell lines (MiaPaCa-Scr, Panc-1 Scr, and BxPC3-Neo) were generated previously (Srivastava *et al*, 2015). For transient transfection of HIF1 α and HuR siRNAs, cells at 50–70% confluence were treated with 100 nM of non-targeting siGENOME™ control pool (siControl, #D-001206-13-05) or ON-TARGETplus SMARTPool siRNAs against HIF1 α (siHIF-1 α , #L-004018-00-0005) or HIF2 α (siHIF2 α , #L-004814-00-0005)

or HuR (siHuR, #L-003773-00-0005) (Dharmacon™) using XtremeGene™ siRNA Transfection Reagent (Roche, Indianapolis, IN) as per manufacturer's instructions. To achieve stable forced expression of HIF1 α in MiaPaCa-shMYB and Panc1-shMYB cells, we transfected them with the pcDNA3-HIF1 α construct (#18949, Addgene) using X-tremeGENE™ HP DNA Transfection Reagent (Roche). Control cells were generated by stable transfection with a pcDNA3-Neo plasmid (#10792, Addgene). The transfected cells were selected in media containing G418/Neomycin (200 μ g/ml). MiaPaCa and BxPC3 cells were maintained in RPMI media (Corning, Glendale, AZ), whereas Panc-1 cells were grown in DMEM media (Corning). Both media were supplemented with 10% fetal bovine serum (Atlanta Biologicals, Lawrenceville, GA, USA) and 100 U/ml penicillin/streptomycin (Sigma-Aldrich). All cell lines were routinely tested for Mycoplasma and authenticated using short tandem repeats genotyping or expression of marker proteins. For hypoxia treatment, cells (2×10^5) were seeded in 60 mm culture dishes, allowed to grow for 24 h, and then subjected to 1.0% O₂ in a hypoxia chamber equipped with an oxygen controller (BioSpherix, Parish, NY) for 0–96 h. For creating hypoxia mimetic condition under normoxia, PC cells were treated with prolyl hydroxylase inhibitors, cobalt chloride (CoCl₂, 100 μ M) or dimethylloxaloylglycine (DMOG, 1 mM) for 6 h. These treatments lead to hypoxia-independent stabilization of HIF1 α and thus are useful in monitoring HIF1 α -dependent gene regulatory and phenotypic responses. However, a limitation of these treatments besides toxicity concerns is that we cannot determine HIF1 α -independent effects of hypoxia (Byrne *et al*, 2014).

RNA extraction and quantitative real-time PCR

Total RNA from cells was extracted using TRIzol reagent (Invitrogen, Carlsbad, CA, USA) and quantified using Nanodrop 1000 (Thermo Scientific). cDNA was synthesized using two μ g of total RNA and a High-Capacity Complementary DNA Reverse Transcription Kit (Thermo Scientific) following the manufacturer's instructions. q-RT PCR was performed using Maxima SYBR Green/ROX qPCR Master Mix kit (Thermo Scientific) on the CFX96™ real-time system (Bio-Rad, Hercules, CA, USA) using gene-specific primer pair sets (Appendix Table S2).

Measurement of mRNA stability and RNA-IP assay

The stability of mRNA was measured as previously described (Zhang *et al*, 2021). In brief, cells were grown to 60–80% confluence in 60 mm dishes and treated with 10 μ g/ml Actinomycin D (Sigma) 1 h before incubation under normoxia or hypoxia (1.0% O₂). Total RNA was isolated at various time intervals and analyzed for HIF1 α mRNA levels using quantitative RT-PCR. RNA immunoprecipitation was performed using an RNA CHIP-IT kit (#53024, Active Motif) following the manufacturer's instructions with slight modifications. Briefly, PC cells (5×10^6 /150-mm dish) were cultured and treated under hypoxia or normoxia for 6 h, and the RNA-protein complex was cross-linked using 1.0% formaldehyde. Cells were then lysed and fractionated into cytoplasmic and nuclei fractions. Cytoplasmic fractions were sonicated (10 cycles of 20 s on/off, 20% amplitude) followed by DNase I treatment and afterward subjected to immunoprecipitation using protein G magnetic beads with either anti-HuR or control anti-IgG antibodies. After overnight incubation at 4°C,

beads were washed sequentially, eluted, and reverse cross-linked at 65°C for 2 h after proteinase K treatment. The RNA was extracted using the Trizol method, and RT-PCR was performed using sets of primers specific for the 3'UTR region of MYB (Appendix Table S3).

Chromatin-immunoprecipitation (ChIP) assay

The binding of MYB and HIF1 α to their target gene promoters was analyzed by performing a ChIP assay as described earlier (Arora *et al*, 2013). Briefly, cells (5×10^6) were cultured in 150 mm dishes to 60–70% confluence and subjected to hypoxia treatment for 6 h. After that, cells were incubated with 1.0% formaldehyde (Sigma) for 10 min to cross-link cellular DNA and proteins, then scraped in an ice-cold cell scraping solution supplemented with protease inhibitors. DNA was enzymatically sheared using ChIP-IT Express Enzymatic Kit (Active Motif, CA, USA) and immunoprecipitated using protein G magnetic beads with anti-MYB or anti-HIF1 α or normal rabbit IgG (control) antibodies by overnight incubation. Magnetic beads were washed, cross-linking reversed in reverse cross-linking buffer, followed by protein digestion using proteinase K and DNA isolation. The purified ChIPed DNA was amplified by PCR using promoter sequence-specific primer sets (Appendix Table S4).

Measurement of cell viability

Cells were trypsinized, stained with 0.4% Trypan Blue (Thermo Fisher Scientific), and counted on Countess Automated Cell Counter (Life Technologies) as described earlier (Patton *et al*, 2020). For direct measurement of live-dead cells, cells were cultured in FluoroDish (#FD35-100, World Precision Instruments, Inc., Sarasota, FL, USA), subjected to hypoxia for 48 h, and then incubated with PBS containing 2 μ M Calcein AM (Invitrogen) and 4 μ M EthD-1 (Invitrogen) dyes for 15 min. After washing with PBS, cells were observed under the fluorescence microscope (Nikon, Lewisville, TX, USA). The dead cells were detected by bright red fluorescence, and live cells were identified by green fluorescence and counted using Image J software as described earlier (Khan *et al*, 2020). The measurement of apoptosis was performed using PE Annexin V Apoptosis Detection Kit (BD Biosciences, San Diego, CA, USA), followed by flow cytometry as described previously (Arora *et al*, 2011). Briefly, 5×10^5 cells were cultured in 60 mm dishes and allowed to grow under normoxia and hypoxia for 48 h; thereafter, cells were harvested and stained with PE Annexin V and 7-AAD for 15 min followed by FACS analysis.

Protein extraction and immunoblot analysis

Total protein was extracted from cells in Pierce™ RIPA Buffer (Thermo Scientific) supplemented with Halt™ Single-Use Cocktail (100 \times) of protease and phosphatase inhibitors (Thermo Scientific). Cytoplasmic and nuclear protein fractions were isolated using NE-PER™ Nuclear and Cytoplasmic Extraction Reagents (Thermo Fisher Scientific, Logan, UT, USA). Protein concentration was estimated using a protein assay kit (Bio-Rad). Following quantification, 60–80 μ g protein (unless specified) was resolved on SDS-PAGE, blotted on PVDF membrane (0.45 μ m) (Thermo Scientific), and protein signals were detected using SuperSignal West Femto Maximum sensitivity substrate kit (Thermo Scientific). Protein bands were

visualized and photographed using a ChemiDoc XRS⁺ system (Bio-Rad Laboratories, Inc., California, USA).

Luciferase promoter-reporter assay

Cells were grown to 50–60% confluence in 6-well plates and transfected with 500 ng of either GLuc-ONTM HIF1 α promoter-reporter plasmid (HPRM39172-PG04, GeneCopoeia, MD, USA) or MYB promoter-reporter luciferase plasmid (HPRM34981-PG02, GeneCopoeia) and Secreted alkaline phosphatase (SEAP) Expression plasmid (SEAP-PA01) or pGL3-MYB-3'UTR (#25798, Addgene) (Navarro *et al.*, 2009). After 24 h, media was replaced, and cells were exposed to hypoxia (1.0% O₂) for 12 h or cultured under normoxic conditions. The conditioned media was collected to measure secretory Gaussia luciferase (GLuc) and Alkaline Phosphatase (SEAP) activities using Secrete-PairTM Dual Luminescence Assay Kit (GeneCopoeia, MD, USA) following the manufacturer's protocol. Gaussia luciferase activity was normalized with SEAP activity to control for transfection efficiency.

Lactate secretion and glucose uptake assay

Cells (1×10^5) were seeded in 6-well plates and grown to 50–60% confluence. After that, the media was replaced, and cells were incubated under hypoxia for 48 h. The conditioned media (CM) was collected and stored at -80°C until further use. The lactate and glucose concentrations in the CM were measured using commercial Lactate (K607-100) and Glucose (K686-100) assay kits (BioVision, CA, USA) following the manufacturer's instructions.

Measurement of extracellular acidification rate and oxygen consumption rate

The basal rates of glycolysis and oxidative phosphorylation were evaluated using the Glycolysis Stress Test kit (# 103020-100, Seahorse Bioscience) and Mito Stress Test kit (#103015-100, Seahorse Bioscience), respectively, on XFe96 Extracellular Flux Analyzer (Seahorse Biosciences). Briefly, cells (10×10^3) were seeded in 96-well XFe96 cell culture plates and allowed to grow for 24 h followed by treatment with CoCl₂ (100 μM) for 16 h. For extracellular acidification rate (ECAR), cells were incubated with fresh media containing glutamine (2 mM) but without serum, glucose, or bicarbonate and incubated in a non-CO₂ incubator for 1 h. At the time of measurement, glucose (10 mM), oligomycin (1 μM), and 2-deoxy-D-glucose (50 mM) were diluted in RPMI media and sequentially loaded into the injection ports of the flux analyzer. For oxygen consumption rate (OCR) determination, cells were incubated with serum-free fresh media containing glutamine (2 mM), glucose (10 mM), and pyruvate (1 mM) for 1 h at 37°C in a non-CO₂ incubator. pH or oxygen-sensitive probes equipped cartridges were pre-incubated with calibration solution overnight in an incubator without CO₂. Time-course analysis of OCR was done before and after injection of ATP synthase complex inhibitor, oligomycin (1 μM), ATP synthesis uncoupler, Carbonyl cyanide-*p*-trifluoromethoxyphenylhydrazone (FCCP, 0.5 μM), and a mixture of complex I inhibitor, rotenone, and complex III inhibitor, antimycin A (0.5 μM) diluted in RPMI and sequentially loaded into injection ports. Three baseline measurements of OCR or ECAR were taken before sequential injection of the reagents or mitochondrial inhibitors. Each

assay was run in one plate with 3–4 replicates and repeated at least thrice. Data were normalized with cell numbers counted in each well using Celigo Image Cytometer (Nexcelom Bioscience LLC, Lawrence, MA, USA).

Extraction of metabolites and quantification by mass spectrometry

Cells (4×10^6) were cultured in 150 mm dishes and incubated under hypoxia for 48 h at subconfluence. Metabolites were extracted as described earlier with slight modifications (Tadi *et al.*, 2013; Gunda *et al.*, 2018). In brief, media was aspirated, and cells were rinsed with MS grade water (ThermoFisher Scientific), followed by the addition of ice-cold 80% methanol and 10 min incubation at -80°C . After that, cells were scraped and further incubated at -80°C for 10 min, followed by thorough vortexing and centrifugation at 3,000 *g* for 10 min at 4°C . The supernatant was collected and lyophilized using a freeze drier until further assay. Lyophilized extracts of metabolites were reconstituted in 10 mM ammonium acetate and injected in Agilent Zorbax 300SB (C18, 2.1×150 mm) Column on Agilent 1200 series LC. Initially, the flow rate used for LC separation was 50 $\mu\text{l}/\text{min}$ for 20 min, which was further ramped to 150 $\mu\text{l}/\text{min}$ until the completion of the run. A gradient of eluent (Eluent A – 10 mM ammonium acetate in 0.1% formic acid and Eluent B – 0.1% formic acid in methanol) was used to separate metabolites. The gradient condition was as follows: 2% eluent B for 20 min, followed by 95% eluent B for 5 min, and 2% eluent B for 15 min. The LC eluent was subjected to a Thermo Qe Orbitrap Mass spectrometer (Thermo Scientific, San Jose, CA, USA) equipped with electrospray ionization. The electrospray ionization spray voltage was 3.5 kV, vaporizer temperature was 300°C , sheath gas N₂ pressure was 20 (arbitrary unit), auxiliary gas pressure was 4 (arbitrary units), and ion sweep gas pressure was 1. The metabolites spectrum data were acquired in negative ionization in SIM mode and processed using Xcalibur software (Thermo Fisher Scientific).

Co-immunoprecipitation

Cells lysates (150 μg , pre-cleared with protein A agarose beads) were incubated with anti-MYB, anti-HIF1 α , anti-p300, or control anti-IgG antibodies (1 μg each) overnight at 4°C followed by incubation with Protein A agarose beads (Thermo Scientific) for 3 h at 4°C . The immunoprecipitated complex was centrifuged and washed with NP-40 lysis buffer. Samples were eluted using elution buffer (primary amine, pH 2.8), mixed with 6 \times sample loading buffer containing 1 M Tris, and subjected to immunoblotting using anti-MYB, -HIF1 α , and -p300 antibodies.

Confocal microscopy

Cells (2.5×10^4) were cultured in FluoroDish (#FD35-100, World Precision Instruments, Inc., Sarasota, FL, USA) for 48 h, followed by incubation under hypoxia for 6 h. After that, cells were washed with $1 \times$ PBS, fixed in 4% paraformaldehyde for 10 min, and incubated with 5% BSA for 60 min for blocking. Cells were then incubated with anti-MYB (#12319S) rabbit monoclonal, anti-HIF1 α (#79233S) mouse monoclonal, anti-HuR (#12582) rabbit monoclonal (Cell Signaling Technology, Danvers, MA, USA), and anti-p300

(#AF3789) goat polyclonal antibodies (R&D system, Minneapolis, MN, USA) at 1:100 dilution for overnight at 4°C. After that, cells were washed with 1× PBS and incubated with secondary antibodies [Alexa Fluor™ 568 (#A11004, anti-mouse, Invitrogen, Carlsbad, CA, USA), Alexa Fluor® 647 (#A21447, anti-goat), and Alexa Fluor 488 (#A11008, anti-rabbit)] (Thermo Scientific, Rockford, IL, USA) for 60 min. Following washing with 1× PBS, cells were mounted with an anti-fade Vectashield mounting medium (Vector Laboratories, Burlingame, CA, USA) and imaged using a Nikon TE2000-E Automated Widefield Microscope equipped with a CoolSnap HQ CCD camera (Nikon Instruments Inc., Melville, NY, USA).

Generation of CRISPR/Cas9 knockout cell lines

Alt-R CRISPR-Cas9 gene-editing system from IDT (Integrated DNA Technologies, Coralville, Iowa, USA) was used to generate MYB knockout pancreatic cancer cells. To prepare sgRNA, two pre-designed Alt-R CRISPR-Cas9 crRNA for MYB, Hs. Cas9.MYB.1.AA (MYB exon 6, positive strand, AGG PAM site, sequence: GAATTC-TACAATGCGTCGGA) and Hs. Cas9.MYB.1.AB (MYB exon 2, positive strand, TGG PAM site sequence: CAAGTCTGGAAAGCGTCACT) were mixed in an equimolar ratio with Alt-R® CRISPR-Cas9 tracrRNA, ATTO™ 550 (#1075928, IDT). After heating at 95°C for 5 min, the reaction mixture was allowed to cool at RT for 1 h, and the Cas9RNP complex was formed by adding sgRNA and purified Cas9 Nuclease V3 enzyme (#1081058) at 1 μM working concentration and incubated for 15 min at 37°C. After that, the transfection complex was prepared by mixing the Cas9RNP complex with Lipofectamine® CRISPRMAX transfection reagent (#CMAX00003, Invitrogen) following the instruction manual and mixed with the cells (3×10^5) in 12-well plates. Cells were allowed to grow for 48 h, followed by single-cell sorting into a 96-well plate based on ATTO™ 550 fluorescence. Positive clones were verified using PCR amplification and Western blotting.

Animal studies

Animal studies were performed after obtaining the necessary approval from the Institutional Animal Care and Use Committee (IACUC). Athymic nude mice (4–6 weeks old) were purchased (Harlan Laboratories, Prattville, AL) and randomly allocated ($n = 6$ in each group) to three experimental groups (MiaPaCa control; MiaPaCa- MYB KO; and MiaPaCa- MYB KO- HIF1 α ^{OE}). After an acclimatization period of 1 week, luciferase-tagged cells (1.0×10^6) were injected into the tail of the pancreas of mice as described previously (Srivastava *et al.*, 2015). All mice were kept in a sterile and comfortable environment and provided food and water *ad libitum*. Mice were monitored daily by the investigating team and the vivarium staff for any signs of pain and distress. An unblinded, non-invasive bioluminescence imaging of mice was performed to observe tumor growth using Xenogen-IVIS-cooled CCD optical system (IVIS Spectrum) after i.p. injection of D-luciferin (150 mg/kg body weight). Hypoxic cell marker, pimonidazole hydrochloride (Hypoxyprobe, Burlington, MA, USA), was injected intraperitoneally into the mice (60 mg/kg body weight) 2 h before sacrificing the animals as described earlier (Guillaumond *et al.*, 2013; Conway *et al.*, 2018). All mice were sacrificed after 5 weeks of tumor cell injection, and tumors were resected, weighed, and their volumes measured using

the following formula: $(A \times B^2)/2$, where A is the larger and B is the smaller of the two dimensions. Levels of glucose, lactate, and citrate metabolites were measured in tumor xenograft tissues using commercial assay kits (#ab169559, #ab65331, and #ab83396) (Abcam, Cambridge, MA, USA). In brief, tissue (~10 mg) was lysed in 500 μl assay buffer using Dounce homogenizer (15–20 strokes) on ice, followed by centrifugation (5 min) at 13,400 g. The supernatant was collected, and glucose, lactate, and citrate metabolites were measured following the manufacturer's protocol.

Immunohistochemistry

The pancreatic tumor xenografts were excised and processed for immunohistochemistry as described previously (Khan *et al.*, 2020). Briefly, tumor tissues were fixed in formalin, embedded in paraffin, and cut into 5-μm thick sections. After deparaffinization, rehydration, and antigen retrieval, endogenous peroxidase activity was blocked by incubating the sections in Peroxidized 1 (#PX968MM; Biocare Medical), followed by blocking in background sniper (#BS966L; Biocare Medical). Tumor sections were then incubated with primary antibodies specific to GLUT3 (anti-rabbit # ab41525), HK2 (anti-rabbit, # ab209847), and MCT4 (anti-mouse, #sc-376140), and pimonidazole adducts (anti-rabbit # HP PAb27) followed by washing and incubation with HRP-labeled secondary antibodies (anti-rabbit #M3R531 and anti-mouse; #M3M530; Biocare Medical). The brown color was developed after adding 3, 3' diaminobenzidine (DAB) substrate (BDB2004L; Biocare Medical). Immunostained sections were scanned, and images were captured using Aperio ScanScope (Leica Biosystems, CA, USA).

Statistical analysis

All the experiments were performed at least three times, and data were analyzed in Excel (Microsoft) or Prism 8.1 (GraphPad) spreadsheets and expressed as mean ± SD. A Student's *t*-test was performed to compare two groups, and one-way ANOVA was used for multiple comparisons. $P < 0.05$ was considered statistically significant.

Data availability

Our study includes no data deposited in external repositories.

Expanded View for this article is available [online](#).

Acknowledgements

We acknowledge the support of Mass Spectrometry, USA Health Biobank Histology, Flow Cytometry, and Bioimaging core facilities of the University of South Alabama. Schematic summary figure was created with [BioRender.com](#). This work was supported, in part, by a grant (R01CA224306 to APS) from the National Cancer Institute (NCI/NIH).

Author contributions

Shashi Anand: Conceptualization; formal analysis; investigation; visualization; methodology; writing – original draft; writing – review and editing.

Mohammad Aslam Khan: Conceptualization; formal analysis; validation; investigation; visualization; methodology; writing – original draft; writing – review and editing. **Haseeb Zubair:** Conceptualization; formal

analysis; investigation; visualization; methodology; writing – review and editing. **Sarabjeet Kour Sudan:** Formal analysis; investigation; visualization; writing – review and editing. **Kunwar Somesh Vikramdeo:** Formal analysis; validation; investigation; writing – review and editing. **Sachin Kumar Deshmukh:** Investigation; writing – review and editing. **Shafquat Azim:** Formal analysis; validation; writing – review and editing. **Sanjeev Kumar Srivastava:** Investigation; writing – review and editing. **Seema Singh:** Writing – review and editing. **Ajay Pratap Singh:** Conceptualization; resources; formal analysis; supervision; funding acquisition; project administration; writing – review and editing.

Disclosure and competing interests statement

The authors declare that they have no conflict of interest.

References

- Arany Z, Huang LE, Eckner R, Bhattacharya S, Jiang C, Goldberg MA, Bunn HF, Livingston DM (1996) An essential role for p300/CBP in the cellular response to hypoxia. *Proc Natl Acad Sci U S A* 93: 12969–12973
- Arora S, Bhardwaj A, Srivastava SK, Singh S, McClellan S, Wang B, Singh AP (2011) Honokiol arrests cell cycle, induces apoptosis, and potentiates the cytotoxic effect of gemcitabine in human pancreatic cancer cells. *PLoS One* 6: e21573
- Arora S, Bhardwaj A, Singh S, Srivastava SK, McClellan S, Nirodi CS, Piazza GA, Grizzle WE, Owen LB, Singh AP (2013) An undesired effect of chemotherapy: gemcitabine promotes pancreatic cancer cell invasiveness through reactive oxygen species-dependent, nuclear factor kappaB- and hypoxia-inducible factor 1alpha-mediated up-regulation of CXCR4. *J Biol Chem* 288: 21197–21207
- Azim S, Zubair H, Srivastava SK, Bhardwaj A, Zubair A, Ahmad A, Singh S, Khushman M, Singh AP (2016) Deep sequencing and *in silico* analyses identify MYB-regulated gene networks and signaling pathways in pancreatic cancer. *Sci Rep* 6: 28446
- Azoitei N, Becher A, Steinestel K, Rouhi A, Diepold K, Genze F, Simmet T, Seufferlein T (2016) PKM2 promotes tumor angiogenesis by regulating HIF-1alpha through NF-kappaB activation. *Mol Cancer* 15: 3
- Bhardwaj A, Srivastava SK, Singh S, Tyagi N, Arora S, Carter JE, Khushman M, Singh AP (2016) MYB promotes desmoplasia in pancreatic cancer through direct transcriptional up-regulation and cooperative action of sonic hedgehog and adrenomedullin. *J Biol Chem* 291: 16263–16270
- Blanco FF, Jimbo M, Wulfschuhle J, Gallagher I, Deng J, Enyenihi L, Meisner-Kober N, Londin E, Rigoutsos I, Sawicki JA *et al* (2016) The mRNA-binding protein HuR promotes hypoxia-induced chemoresistance through posttranscriptional regulation of the proto-oncogene PIM1 in pancreatic cancer cells. *Oncogene* 35: 2529–2541
- Byrne MB, Leslie MT, Gaskins HR, Kenis PJA (2014) Methods to study the tumor microenvironment under controlled oxygen conditions. *Trends Biotechnol* 32: 556–563
- Choudhry H, Harris AL (2018) Advances in hypoxia-inducible factor biology. *Cell Metab* 27: 281–298
- Conway JRW, Warren SC, Herrmann D, Murphy KJ, Cazet AS, Vennin C, Shearer RF, Killen MJ, Magenau A, Melenc P *et al* (2018) Intravital imaging to monitor therapeutic response in moving hypoxic regions resistant to PI3K pathway targeting in pancreatic cancer. *Cell Rep* 23: 3312–3326
- Costantino CL, Witkiewicz AK, Kuwano Y, Cozzitorto JA, Kennedy EP, Dasgupta A, Keen JC, Yeo CJ, Gorospe M, Brody JR (2009) The role of HuR in gemcitabine efficacy in pancreatic cancer: HuR up-regulates the expression of the gemcitabine metabolizing enzyme deoxycytidine kinase. *Cancer Res* 69: 4567–4572
- Dasse E, Volpe G, Walton DS, Wilson N, Del Pozzo W, O'Neill LP, Slany RK, Frampton J, Dumon S (2012) Distinct regulation of c-myc gene expression by HoxA9, Meis1 and Pbx proteins in normal hematopoietic progenitors and transformed myeloid cells. *Blood Cancer J* 2: e76
- Dauer P, Nomura A, Saluja A, Banerjee S (2017) Microenvironment in determining chemo-resistance in pancreatic cancer: neighborhood matters. *Pancreatology* 17: 7–12
- Dengler VL, Galbraith M, Espinosa JM (2014) Transcriptional regulation by hypoxia inducible factors. *Crit Rev Biochem Mol Biol* 49: 1–15
- Denko NC (2008) Hypoxia, HIF1 and glucose metabolism in the solid tumour. *Nat Rev Cancer* 8: 705–713
- Eales KL, Hollinshead KE, Tennant DA (2016) Hypoxia and metabolic adaptation of cancer cells. *Oncogene* 35: e190
- Elcheva IA, Wood T, Chiarolanzio K, Chim B, Wong M, Singh V, Gowda CP, Lu Q, Hafner M, Dovat S *et al* (2020) RNA-binding protein IGF2BP1 maintains leukemia stem cell properties by regulating HOXB4, MYB, and ALDH1A1. *Leukemia* 34: 1354–1363
- Favaro E, Bensaad K, Chong MG, Tennant DA, Ferguson DJ, Snell C, Steers G, Turley H, Li JL, Gunther UL *et al* (2012) Glucose utilization via glycogen phosphorylase sustains proliferation and prevents premature senescence in cancer cells. *Cell Metab* 16: 751–764
- Feig C, Gopinathan A, Neesse A, Chan DS, Cook N, Tuveson DA (2012) The pancreas cancer microenvironment. *Clin Cancer Res* 18: 4266–4276
- Fuglerud BM, Ledsaak M, Rogne M, Eskeland R, Gabrielsen OS (2018) The pioneer factor activity of c-Myb involves recruitment of p300 and induction of histone acetylation followed by acetylation-induced chromatin dissociation. *Epigenetics Chromatin* 11: 35
- George OL, Ness SA (2014) Situational awareness: regulation of the myb transcription factor in differentiation, the cell cycle and oncogenesis. *Cancers (Basel)* 6: 2049–2071
- Greig KT, Carotta S, Nutt SL (2008) Critical roles for c-Myb in hematopoietic progenitor cells. *Semin Immunol* 20: 247–256
- Gudas JM, Klein RC, Oka M, Cowan KH (1995) Posttranscriptional regulation of the c-myc proto-oncogene in estrogen receptor-positive breast cancer cells. *Clin Cancer Res* 1: 235–243
- Guillaumond F, Leca J, Olivares O, Lavaut MN, Vidal N, Berthezene P, Dusetti NJ, Loncle C, Calvo E, Turrini O *et al* (2013) Strengthened glycolysis under hypoxia supports tumor symbiosis and hexosamine biosynthesis in pancreatic adenocarcinoma. *Proc Natl Acad Sci U S A* 110: 3919–3924
- Gunda V, Kumar S, Dasgupta A, Singh PK (2018) Hypoxia-induced metabolomic alterations in pancreatic cancer cells. *Methods Mol Biol* 1742: 95–105
- Heinonen M, Bono P, Narko K, Chang SH, Lundin J, Joensuu H, Furneaux H, Hla T, Haglund C, Ristimaki A (2005) Cytoplasmic HuR expression is a prognostic factor in invasive ductal breast carcinoma. *Cancer Res* 65: 2157–2161
- Hingorani SR, Petricoin EF, Maitra A, Rajapakse V, King C, Jacobetz MA, Ross S, Conrads TP, Veenstra TD, Hitt BA *et al* (2003) Preinvasive and invasive ductal pancreatic cancer and its early detection in the mouse. *Cancer Cell* 4: 437–450
- Hollinshead KER, Parker SJ, Eapen VV, Encarnacion-Rosado J, Sohn A, Oncu T, Cammer M, Mancias JD, Kimmelman AC (2020) Respiratory Supercomplexes promote mitochondrial efficiency and growth in severely hypoxic pancreatic cancer. *Cell Rep* 33: 108231
- Jiang P, Du W, Wu M (2014) Regulation of the pentose phosphate pathway in cancer. *Protein Cell* 5: 592–602

- Jochmanova I, Pacak K (2016) Pheochromocytoma: the first metabolic endocrine cancer. *Clin Cancer Res* 22: 5001–5011
- Kasper LH, Boussouar F, Ney PA, Jackson CW, Rehg J, van Deursen JM, Brindle PK (2002) A transcription-factor-binding surface of coactivator p300 is required for haematopoiesis. *Nature* 419: 738–743
- Khan MA, Srivastava SK, Zubair H, Patel GK, Arora S, Khushman M, Carter JE, Gorman GS, Singh S, Singh AP (2020) Co-targeting of CXCR4 and hedgehog pathways disrupts tumor-stromal crosstalk and improves chemotherapeutic efficacy in pancreatic cancer. *J Biol Chem* 295: 8413–8424
- Kim Y, Nam HJ, Lee J, Park DY, Kim C, Yu YS, Kim D, Park SW, Bhin J, Hwang D et al (2016) Methylation-dependent regulation of HIF-1alpha stability restricts retinal and tumour angiogenesis. *Nat Commun* 7: 10347
- Lee P, Chandel NS, Simon MC (2020) Cellular adaptation to hypoxia through hypoxia inducible factors and beyond. *Nat Rev Mol Cell Biol* 21: 268–283
- Li L, Chang W, Yang G, Ren C, Park S, Karantanos T, Karanika S, Wang J, Yin J, Shah PK et al (2014) Targeting poly(ADP-ribose) polymerase and the c-Myb-regulated DNA damage response pathway in castration-resistant prostate cancer. *Sci Signal* 7: ra47
- Li Y, Jin K, van Pelt GW, van Dam H, Yu X, Mesker WE, Ten Dijke P, Zhou F, Zhang L (2016) c-Myb enhances breast cancer invasion and metastasis through the Wnt/beta-catenin/Axin2 pathway. *Cancer Res* 76: 3364–3375
- Liu X, Gold KA, Dmitrovsky E (2015) The Myb-p300 interaction is a novel molecular pharmacologic target. *Mol Cancer Ther* 14: 1273–1275
- Majmundar AJ, Wong WJ, Simon MC (2010) Hypoxia-inducible factors and the response to hypoxic stress. *Mol Cell* 40: 294–309
- Marin-Hernandez A, Gallardo-Perez JC, Ralph SJ, Rodriguez-Enriquez S, Moreno-Sanchez R (2009) HIF-1alpha modulates energy metabolism in cancer cells by inducing over-expression of specific glycolytic isoforms. *Mini Rev Med Chem* 9: 1084–1101
- Messeguer X, Escudero R, Farre D, Nunez O, Martinez J, Alba MM (2002) PROMO: detection of known transcription regulatory elements using species-tailored searches. *Bioinformatics* 18: 333–334
- Mets E, van der Meulen J, van Peer G, Boice M, Mestdagh P, van de Walle I, Lammens T, Goossens S, de Moerloose B, Benoit Y et al (2015) MicroRNA-193b-3p acts as a tumor suppressor by targeting the MYB oncogene in T-cell acute lymphoblastic leukemia. *Leukemia* 29: 798–806
- Mrena J, Wiksten JP, Thiel A, Korkola A, Pohjola L, Lundin J, Nordling S, Ristimaki A, Haglund C (2005) Cyclooxygenase-2 is an independent prognostic factor in gastric cancer and its expression is regulated by the messenger RNA stability factor HuR. *Clin Cancer Res* 11: 7362–7368
- Navarro F, Gutman D, Meire E, Caceres M, Rigoutsos I, Bentwich Z, Lieberman J (2009) miR-34a contributes to megakaryocytic differentiation of K562 cells independently of p53. *Blood* 114: 2181–2192
- Pan H, Strickland A, Madhu V, Johnson ZI, Chand SN, Brody JR, Fertala A, Zheng Z, Shapiro IM, Risbud MV (2019) RNA binding protein HuR regulates extracellular matrix gene expression and pH homeostasis independent of controlling HIF-1alpha signaling in nucleus pulposus cells. *Matrix Biol* 77: 23–40
- Patton MC, Zubair H, Khan MA, Singh S, Singh AP (2020) Hypoxia alters the release and size distribution of extracellular vesicles in pancreatic cancer cells to support their adaptive survival. *J Cell Biochem* 121: 828–839
- Pawlus MR, Wang L, Hu CJ (2014) STAT3 and HIF1alpha cooperatively activate HIF1 target genes in MDA-MB-231 and RCC4 cells. *Oncogene* 33: 1670–1679
- Peng W, Furuuchi N, Aslanukova L, Huang YH, Brown SZ, Jiang W, Addya S, Vishwakarma V, Peters E, Brody JR et al (2018) Elevated HuR in pancreas promotes a pancreatitis-like inflammatory microenvironment that facilitates tumor development. *Mol Cell Biol* 38: e00427-17
- Petrova V, Annicchiarico-Petruzzelli M, Melino G, Amelio I (2018) The hypoxic tumour microenvironment. *Oncogene* 7: 10
- Reglero C, Lafarga V, Rivas V, Albitre A, Ramos P, Berciano SR, Tapia O, Martinez-Chantar ML, Mayor F Jr, Penela P (2020) GRK2-dependent HuR phosphorylation regulates HIF1alpha activation under hypoxia or adrenergic stress. *Cancers (Basel)* 12: 1216
- Rousset M, Zweibaum A, Fogh J (1981) Presence of glycogen and growth-related variations in 58 cultured human tumor cell lines of various tissue origins. *Cancer Res* 41: 1165–1170
- Salceda S, Caro J (1997) Hypoxia-inducible factor 1alpha (HIF-1alpha) protein is rapidly degraded by the ubiquitin-proteasome system under normoxic conditions. Its stabilization by hypoxia depends on redox-induced changes. *J Biol Chem* 272: 22642–22647
- Semenza GL (2010) Defining the role of hypoxia-inducible factor 1 in cancer biology and therapeutics. *Oncogene* 29: 625–634
- Semenza GL (2013) HIF-1 mediates metabolic responses to intratumoral hypoxia and oncogenic mutations. *J Clin Invest* 123: 3664–3671
- Shen C, Beroukhi R, Schumacher SE, Zhou J, Chang M, Signoretti S, Kaelin WG Jr (2011) Genetic and functional studies implicate HIF1alpha as a 14q kidney cancer suppressor gene. *Cancer Discov* 1: 222–235
- Siegel RL, Miller KD, Fuchs HE, Jemal A (2022) Cancer statistics, 2022. *CA Cancer J Clin* 72: 7–33
- Singh AP, Arora S, Bhardwaj A, Srivastava SK, Kadakia MP, Wang B, Grizzle WE, Owen LB, Singh S (2012) CXCL12/CXCR4 protein signaling axis induces sonic hedgehog expression in pancreatic cancer cells via extracellular regulated kinase- and Akt kinase-mediated activation of nuclear factor kappaB: implications for bidirectional tumor-stromal interactions. *J Biol Chem* 287: 39115–39124
- Slamon DJ, Boone TC, Murdock DC, Keith DE, Press MF, Larson RA, Souza LM (1986) Studies of the human c-myc gene and its product in human acute leukemias. *Science* 233: 347–351
- Srivastava SK, Bhardwaj A, Arora S, Singh S, Azim S, Tyagi N, Carter JE, Wang B, Singh AP (2015) MYB is a novel regulator of pancreatic tumour growth and metastasis. *Br J Cancer* 113: 1694–1703
- Srivastava SK, Khan MA, Anand S, Zubair H, Deshmukh SK, Patel GK, Singh S, Andrews J, Wang B, Carter JE et al (2021) MYB interacts with androgen receptor, sustains its ligand-independent activation and promotes castration resistance in prostate cancer. *Br J Cancer* 126: 1205–1214
- Tadi S, Kim SJ, Ryu MJ, Jeong J-S, Kweon GR, Shong M, Yim Y-H (2013) Metabolic rebalancing of CR6 interaction factor 1-deficient mouse embryonic fibroblasts: a mass spectrometry-based metabolic analysis. *Bull Korean Chem Soc* 34: 35–41
- Tiwari A, Tashiro K, Dixit A, Soni A, Vogel K, Hall B, Shafqat I, Slaughter J, Param N, Le A et al (2020) Loss of HIF1A from pancreatic cancer cells increases expression of PPP1R1B and degradation of p53 to promote invasion and metastasis. *Gastroenterology* 159: 1882–1897
- Tsunoda T, Takagi T (1999) Estimating transcription factor bindability on DNA. *Bioinformatics* 15: 622–630
- Wallrapp C, Muller-Pillasch F, Solinas-Toldo S, Lichter P, Friess H, Buchler M, Fink T, Adler G, Gress TM (1997) Characterization of a high copy number amplification at 6q24 in pancreatic cancer identifies c-myc as a candidate oncogene. *Cancer Res* 57: 3135–3139
- Wang J, Guo Y, Chu H, Guan Y, Bi J, Wang B (2013) Multiple functions of the RNA-binding protein HuR in cancer progression, treatment responses and prognosis. *Int J Mol Sci* 14: 10015–10041

- Wang Y, Lyu Y, Tu K, Xu Q, Yang Y, Salman S, Le N, Lu H, Chen C, Zhu Y *et al* (2021) Histone citrullination by PADI4 is required for HIF-dependent transcriptional responses to hypoxia and tumor vascularization. *Sci Adv* 7: eabe3771
- Weston K (1999) Reassessing the role of C-MYB in tumorigenesis. *Oncogene* 18: 3034–3038
- Wierenga ATJ, Cunningham A, Erdem A, Lopera NV, Brouwers-Vos AZ, Pruis M, Mulder AB, Gunther UL, Martens JHA, Vellenga E *et al* (2019) HIF1/2-exerted control over glycolytic gene expression is not functionally relevant for glycolysis in human leukemic stem/progenitor cells. *Cancer Metab* 7: 11
- Xiao C, Calado DP, Galler G, Thai TH, Patterson HC, Wang J, Rajewsky N, Bender TP, Rajewsky K (2007) MiR-150 controls B cell differentiation by targeting the transcription factor c-Myb. *Cell* 131: 146–159
- Xu R, Yang J, Ren B, Wang H, Yang G, Chen Y, You L, Zhao Y (2020) Reprogramming of amino acid metabolism in pancreatic cancer: recent advances and therapeutic strategies. *Front Oncol* 10: 572722
- Yamasaki A, Yanai K, Onishi H (2020) Hypoxia and pancreatic ductal adenocarcinoma. *Cancer Lett* 484: 9–15
- Zhang H, Zhao X, Guo Y, Chen R, He J, Li L, Qiang Z, Yang Q, Liu X, Huang C *et al* (2021) Hypoxia regulates overall mRNA homeostasis by inducing met (1)-linked linear ubiquitination of AGO2 in cancer cells. *Nat Commun* 12: 5416
- Zubair H, Patel GK, Khan MA, Azim S, Zubair A, Singh S, Srivastava SK, Singh AP (2020) Proteomic analysis of MYB-regulated Secretome identifies functional pathways and biomarkers: potential pathobiological and clinical implications. *J Proteome Res* 19: 794–804